



LUND UNIVERSITY

Convection-diffusion-reaction models of sedimentation

Numerical approximation, analysis of solutions and inverse problems

Careaga, Julio

2021

Document Version:

Publisher's PDF, also known as Version of record

[Link to publication](#)

Citation for published version (APA):

Careaga, J. (2021). *Convection-diffusion-reaction models of sedimentation: Numerical approximation, analysis of solutions and inverse problems*. Department of Mathematical Sciences, Lund University.

Total number of authors:

1

General rights

Unless other specific re-use rights are stated the following general rights apply:

Copyright and moral rights for the publications made accessible in the public portal are retained by the authors and/or other copyright owners and it is a condition of accessing publications that users recognise and abide by the legal requirements associated with these rights.

- Users may download and print one copy of any publication from the public portal for the purpose of private study or research.
- You may not further distribute the material or use it for any profit-making activity or commercial gain
- You may freely distribute the URL identifying the publication in the public portal

Read more about Creative commons licenses: <https://creativecommons.org/licenses/>

Take down policy

If you believe that this document breaches copyright please contact us providing details, and we will remove access to the work immediately and investigate your claim.

LUND UNIVERSITY

PO Box 117
221 00 Lund
+46 46-222 00 00

Convection-diffusion-reaction models of sedimentation:

Numerical approximation, analysis of solutions and inverse problems

by

Julio Careaga



LUND
UNIVERSITY

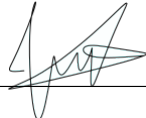
ACADEMIC THESIS

which, by due permission of the Faculty of Engineering at Lund University will be publicly defended on Friday 1st of October, 2021, at 13:00 in room MH:Rieszsalen at the Centre for Mathematical Sciences, Sölvegatan 18, Lund, for the degree of Doctor of Philosophy in Engineering.

Faculty opponent: Professor Steiner Evje, University of Stavanger, Norway.

Organization Centre for Mathematical Sciences Faculty of Engineering Lund University Author: Julio Careaga		Document name DOCTORAL DISSERTATION IN MATHEMATICAL SCIENCES	
		Date of issue October 2021	
		Sponsoring organization	
Title and subtitle Convection-diffusion-reaction models of sedimentation: Numerical approximation, analysis of solutions and inverse problems			
Abstract <p>The core of this Doctoral thesis is mainly based in the studies of one-dimensional initial-boundary value problems, which are given by a single non-linear hyperbolic partial differential equation (PDE) with non-convex flux function, or by a system of strongly degenerate parabolic PDEs, for the simulation of sedimentation processes of solid particles immersed in a fluid. Particular attention is paid to the case of settling in vessels with varying cross-sectional area. Sedimentation processes are widely used in wastewater treatment (WWT) and mineral processing, where accurate model calibration and reliable simulators are needed. Among the topics covered in the research presented in this thesis are the construction of entropy solutions, the development and implementation of reliable numerical schemes for hyperbolic PDEs (and systems of PDEs), the solution of inverse problems of flux identification, and the dissemination of results to the applied sciences.</p> <p>The outputs of this thesis can be divided into three parts. The first part (Papers I to III) contains the construction of the entropy solutions for the PDE modeling the batch sedimentation in vessels with non-constant cross-sectional area (Paper I and II) and for the PDE modeling centrifugal sedimentation (Paper III). The problem is in both cases solved by the method of characteristics and the types of solutions are distinguished mainly depending on the initial value. Paper II contains the description and solution of the inverse problem of flux identification for the model of sedimentation in conical vessels due to gravity, and Paper III the inverse problem for the model of centrifugal settling. In both cases, the solution of the inverse problem has the advantage that almost the entire flux function can be identified from only one experiment. These identification methods mean a significant advantage in comparison with the classic one, made by standard tests in cylindrical vessels, in terms of the portion of flux identified. An algorithm necessary for the identification from discrete data is also presented in each problem (Papers II and III).</p> <p>The second part (Papers IV to VI) includes the development of numerical methods for the simulation of sedimentation in WWT. In Paper IV, a numerical scheme for the case of continuous and batch sedimentation in vessels with varying cross-sectional area is studied. An advantageous CFL condition is derived as an improvement over other numerical methods for the same kind of application. Simulations of continuous and batch settling are also included. Papers V and VI consider reactive settling, where the unknown is a vector of solid and liquid components, and each model is described by a coupled system of convection-diffusion-reaction PDEs. In Paper V, a method-of-lines formulation for the approximation of the model equations is introduced. This formulation has the advantage that it can be solved by any time stepping solver, such as those commonly used in the WWT community where ordinary differential equations (ODEs) should be solved simultaneously with the PDE system. Additionally, an invariant-region property is proved for the scheme and simulations of interesting scenarios are presented. In Paper VI, sequencing batch reactors (SBRs) are studied. The model equations for the SBRs are derived following Paper V, but with the addition that in this case, the extraction and filling of mixture lead to a moving-boundary problem. The movement of the boundary is described by an ODE which can be precomputed. A reliable numerical scheme that preserves the mass is proposed and numerical simulations for the case of denitrification are shown.</p> <p>The third part (Papers VII and VIII) is related to applications and dissemination of the flux identification methods to the applied sciences. The validation of the inverse problem for batch settling in conical vessels is presented in Paper VII. The validation was carried out with data taken from activated sludge collected from the WWT plant in Västerås, Sweden. Paper VIII contains a review of flux identification methods related to PDE models for sedimentation processes. Advantages and disadvantages are discussed, and simulations of identified fluxes with the methods under study are presented.</p> <p>In Chapter 4 the numerical simulation of multidimensional batch sedimentation is discussed and two-dimensional simulations are presented.</p>			
Key words: conservation law; method of characteristics; numerical scheme; continuous sedimentation; inverse problem			
Classification system and/or index terms (if any)			
Supplementary bibliographical information		Language English	
ISSN and key title 1404-0034		ISBN 978-91-7895-970-9	
Recipient's notes		Number of pages 248	Price
		Security classification	

I, the undersigned, being the copyright owner of the abstract of the above-mentioned dissertation, hereby grant to all reference sources the permission to publish and disseminate the abstract of the above-mentioned dissertation.

Signature 

Date 2021-08-13

Convection-diffusion-reaction
models of sedimentation:
Numerical approximation, analysis of
solutions and inverse problems

Doctoral thesis by
Julio Careaga



LUND
UNIVERSITY

Faculty of Engineering
Centre for Mathematical Sciences
Mathematics

Mathematics
Centre for Mathematical Sciences
Lund University
Box 118
SE-221 00 Lund
Sweden

<http://www.maths.lth.se/>

Doctoral Theses in Mathematical Sciences 2021:8
ISSN 1404-0034

ISBN 978-91-7895-970-9 (print)
ISBN 978-91-7895-969-3 (electronic)
LUTFMA-1074-2021

©Julio Careaga, 2021

Printed in Sweden by Media-Tryck, Lund University, Lund 2021

Abstract

The core of this Doctoral thesis is mainly based in the studies of one-dimensional initial-boundary value problems, which are given by a single non-linear hyperbolic partial differential equation (PDE) with non-convex flux function, or by a system of strongly degenerate parabolic PDEs, for the simulation of sedimentation processes of solid particles immersed in a fluid. Particular attention is paid to the case of settling in vessels with varying cross-sectional area. Sedimentation processes are widely used in wastewater treatment (WWT) and mineral processing, where accurate model calibration and reliable simulators are needed. Among the topics covered in the research presented in this thesis are the construction of entropy solutions, the development and implementation of reliable numerical schemes for hyperbolic PDEs (and systems of PDEs), the solution of inverse problems of flux identification, and the dissemination of results to the applied sciences.

The outputs of this thesis can be divided into three parts. The first part (Papers I to III) contains the construction of the entropy solutions for the PDE modeling the batch sedimentation in vessels with non-constant cross-sectional area (Paper I and II) and for the PDE modeling centrifugal sedimentation (Paper III). The problem is in both cases solved by the method of characteristics and the types of solutions are distinguished mainly depending on the initial value. Paper II contains the description and solution of the inverse problem of flux identification for the model of sedimentation in conical vessels due to gravity, and Paper III the inverse problem for the model of centrifugal settling. In both cases, the solution of the inverse problem has the advantage that almost the entire flux function can be identified from only one experiment. These identification methods mean a significant advantage in comparison with the classic one, made by standard tests in cylindrical vessels, in terms of the portion of flux identified. An algorithm necessary for the identification from discrete data is also presented in each problem (Papers II and III).

The second part (Papers IV to VI) includes the development of numerical methods for the simulation of sedimentation in WWT. In Paper IV, a numerical scheme for the

case of continuous and batch sedimentation in vessels with varying cross-sectional area is studied. An advantageous CFL condition is derived as an improvement over other numerical methods for the same kind of application. Simulations of continuous and batch settling are also included. Papers V and VI consider reactive settling, where the unknown is a vector of solid and liquid components, and each model is described by a coupled system of convection-diffusion-reaction PDEs. In Paper V, a method-of-lines formulation for the approximation of the model equations is introduced. This formulation has the advantage that it can be solved by any time stepping solver, such as those commonly used in the WWT community where ordinary differential equations (ODEs) should be solved simultaneously with the PDE system. Additionally, an invariant-region property is proved for the scheme and simulations of interesting scenarios are presented. In Paper VI, sequencing batch reactors (SBRs) are studied. The model equations for the SBRs are derived following Paper V, but with the addition that in this case, the extraction and filling of mixture lead to a moving-boundary problem. The movement of the boundary is described by an ODE which can be precomputed. A reliable numerical scheme that preserves the mass is proposed and numerical simulations for the case of denitrification are shown.

The third part (Papers VII and VIII) is related to applications and dissemination of the flux identification methods to the applied sciences. The validation of the inverse problem for batch settling in conical vessels is presented in Paper VII. The validation was carried out with data taken from activated sludge collected from the WWT plant in Västerås, Sweden. Paper VIII contains a review of flux identification methods related to PDE models for sedimentation processes. Advantages and disadvantages are discussed, and simulations of identified fluxes with the methods under study are presented.

In Chapter 4 the numerical simulation of multidimensional batch sedimentation is discussed and two-dimensional simulations are presented.

Popular Science Summary

The separation of solid particles from a mixture in a fluid due to a specific force (gravity or centrifugal) is called sedimentation or settling, and is present in many natural processes, for example in alluvium, moraines (accumulation of unconsolidated debris in glaciers), the formation of rocks or in reefs at the bottom of the ocean, but it can also be seen in daylife, for instance, in a bottle of juice at the supermarket or in a forgotten cup of coffee that with the past of days the particles of coffee slowly tend to separate from the water.

This process is exploited in many industries. In mineral processing, the separation is carried out in so-called thickeners, which are huge tanks where the main purpose is to separate solid mineral from ore and water. Another application that widely utilizes sedimentation is wastewater treatment, where in the Secondary Settling Tanks the sedimentation due to gravity is applied to separate solid biomass from clean water. In both cases sedimentation is carried out on a large scale, and driven mainly by gravity. But not only big scale processes utilize this principle, blood fractionation due to centrifugation is a common separation process in blood tests. These applications motivate the study of mathematical models for simulation which is one main motivation of this thesis.

The first step in mathematical modeling is the introduction of variables (physical quantities of interest) and equations, but also the assumptions and restrictions to be considered in the model. In the case of modeling sedimentation processes the set of equations are obtained from physical laws: these are partial differential equations (PDEs), which are equations that measure the variations of physical quantities with respect to time and space. The PDEs represent a rich source of interesting mathematical problems, such as the ones treated in this thesis. Some of the questions related to PDE models are, for example, the existence and uniqueness of solutions. For most of the PDEs, as in the case of models for settling processes, solutions are practically impossible to obtain by pen and paper, hence approximate solutions are desirable. The computational approximations of PDEs are carried out by iterative

algorithms called numerical schemes. This thesis is also dedicated to develop reliable numerical schemes, which means that proofs of mathematical properties and theorems about the schemes have to be carried out. Furthermore, computational simulations of scenarios of interest made with the developed mathematical models are included.

Another topic included in this thesis is the inverse problem of “finding” the flux function in the model of sedimentation which describes the flux of the solid particles depending on its local concentration. Inverse problems, as its name says, are problems defined contrariwise; given a part of the solution, for example, experimental data from a laboratory, identify one or more functions that are part of the model. The inverse problems presented in this thesis play an important role as a bridge between the mathematical models (theory) and the concrete applications (reality). They are needed in the calibration step of the modeling. By calibration is here not only meant parameter estimation, but finding an entire unknown function.

Dissemination of mathematical results to the scientific community other than mathematics is an important task when working with applied problems. This has been done via conferences and publications in journals of water and chemical engineering with validation of the inverse problem with real data and simulations of different scenarios.

List of Papers

This thesis is based on the following papers. They are ordered with roman numbers and organized into three parts depending on the topic.

First part: Entropy solutions and inverse problem

- I. R. Bürger, J. Careaga and S. Diehl. Entropy solutions of a scalar conservation law modeling sedimentation in vessels with varying cross-sectional area, *SIAM J. Appl. Math.* 77 (2017), 789–811.
<https://doi.org/10.1137/16M1083177>
- II. R. Bürger, J. Careaga and S. Diehl. Flux identification of scalar conservation laws from sedimentation in a cone, *IMA J. Appl. Math.* 83 (2018), 526–552.
<https://doi.org/10.1093/imamat/hxy018>
- III. J. Careaga and S. Diehl. Entropy solutions and flux identification of a scalar conservation law modelling centrifugal sedimentation, *Math. Meth. Appl. Sci.* (2020), 1–28.
<https://doi.org/10.1002/mma.6212>

Second part: Numerical schemes and simulation models

- IV. R. Bürger, J. Careaga and S. Diehl. A simulation model for settling tanks with varying cross-sectional area, *Chem. Eng. Commun.* 204 (2017), 1270–1281.
<https://doi.org/10.1080/00986445.2017.1360871>
- V. R. Bürger, J. Careaga and S. Diehl. A method-of-lines formulation for a model of reactive settling in tanks with varying cross-sectional area, *IMA J. Appl. Math.* 86 (2021), 514–546.
<https://doi.org/10.1093/imamat/hxab012>
- VI. R. Bürger, J. Careaga, S. Diehl and R. Pineda. A moving-boundary model for reactive settling in wastewater treatment, submitted (2021).
<https://arxiv.org/abs/2105.10961>

Third part: Validation and dissemination

- VII. R. Bürger, J. Careaga, S. Diehl, R. Merckel and J. Zambrano. Estimating the hindered-settling flux function from a batch test in a cone, *Chem. Eng. Sci.* 192 (2018), 244–253.
<https://doi.org/10.1016/j.ces.2018.07.029>
- VIII. R. Bürger, J. Careaga and S. Diehl. A review of flux identification methods for models of sedimentation, *Water Sci. Tech.* 81 (2020), 1715–1722.
<https://doi.org/10.2166/wst.2020.113>

The papers above are reproduced in the printed version of this thesis with permission from the respective publishers.

Subsidiary papers

- IX. R. Bürger, J. Careaga, S. Diehl, C. Mejías, I. Nopens, E. Torfs and P.A. Vanrolleghem. Simulations of reactive settling of activated sludge with a reduced biokinetic model, *Comp. Chem. Eng.* 92 (2016), 216–229.
<https://doi.org/10.1016/j.compchemeng.2016.04.037>
- X. R. Bürger, J. Careaga, S. Diehl, C. Mejías and R. Ruiz-Baier. Convection-diffusion-reaction and transport-flow problems motivated by models of sedimentation: some recent advances, *Proceedings of the International Congress of Mathematicians, Rio de Janeiro*, vol. 3 (2018), 3489–3514.
https://doi.org/10.1142/9789813272880_0189
ISBN: 978-981-3272-87-3
- XI. R. Bürger, J. Careaga and S. Diehl. Flux identification methods of sedimentation, *10th IWA Symposium on Systems Analysis and Integrated Assessment (Watermatex)*, 1-4 September, 2019. Copenhagen, Denmark, 2019.
<https://www.watermatex2019.org/>

Author's contribution

- I. Actively participated in the analysis, contributed introducing a generalization of the cross-sectional area function, implemented the numerical scheme that computes all the characteristic curves and regions, and produced all simulations.
- II. Contributed in solving the inverse problem, wrote parts of the text, made the adapted least-squares method used, implemented the two methods of identification (explicit and parametric), and produced all simulations and figures.
- III. Formulated the project, developed the main results, produced the numerical simulations and all the illustrations, and wrote a substantial part of the text. *Corresponding author.*
- IV. Formulated the project, suggested an improved CFL condition, implemented the numerical method, produced all simulations and wrote most of the text. *Corresponding author.*
- V. Formulated the project, contributed in the development of the numerical scheme, proved the main mathematical result of the paper, and produced all the numerical examples. *Corresponding author.*
- VI. Contributed in the developing of the numerical scheme, participate actively in the discussion, wrote part of the text and produced some of the illustrations.
- VII. Implemented the programming of the identification method for each experiment, wrote parts of the text and produced all simulations. *Corresponding author.*
- VIII. Implemented all the numerical schemes of the different methods presented and produced all the simulations and illustrations of the paper, also contributed in the discussion.

Acknowledgements

I would like to express my special thanks of gratitude to my supervisor, Stefan Diehl, for doing an excellent and highly valuable work of supervision of my doctoral studies. This thesis and all the results obtained would have not been achieved without his constant support, willingness, helpful suggestions and fruitful discussions. Thank you for trusting in my aptitudes and bringing me to the world of research. I also wish to thank the valuable support of my co-advisor Prof. Raimund Bürger who has continually helped me in developing my research. And thanks to my co-advisor Prof. Eskil Hansen for also being part of this project.

I would also like to thank my family, Adelaida, Felipe, Carmen and Oscar, and close friends which represent a fundamental pillar in my life, all of you have always supported and encouraged me to keep forward in life.

And to my fellows at Matematikcentrum with whom I shared the fika everyday and new friends I have met in Sweden, with special mention to Sergio and Maria Silva-Nilsson, thanks to all of you for bringing joy and good vibes to my life in this important challenge.

In addition, I wish to thank one of my former professors at Universidad de Concepción, Freddy Paiva, for all the knowledge I have acquired from him and his confidence in my scientific career. To Prof. Gabriel Gatica for the support I received during my stay at the Center for Research in Mathematical Engineering (CI²MA), Concepción, Chile.

I also want to express my gratitude to Ricardo Ruiz-Baier, from the School of Mathematics at Monash University, Australia, for the invitation and kind hospitality I received during my visit at University of Oxford.

Julio Careaga, Lund, 2021

Contents

1	Introduction	1
1.1	The sedimentation process	1
1.2	Motivation for modeling	2
1.3	Research questions	3
1.4	Previous works	4
1.5	Overview of the new results of this thesis	9
2	Model equations for sedimentation	11
2.1	Model equations in 3D	11
2.2	One-dimensional approach	15
3	Overview and main results of the papers	20
3.1	Exact solutions and inverse problem	20
3.2	Numerical schemes and simulation models	25
3.3	Applications and dissemination	28
4	Two-dimensional numerical simulations	30
4.1	Simplified batch settling	30
4.2	Simplified centrifugal settling in tubes	36
4.3	Fully coupled multidimensional settling	37
	Bibliography	45

Chapter 1

Introduction

1.1 The sedimentation process

Sedimentation processes play an important role in many industrial operations and nature. Some of the applications are related to chemical industry, food industry, blood tests (medicine, biomedical tests), brewing, paper manufacturing, rock formation, petroleum industry, oil industry, mineral processing and wastewater treatment plants [25, 31, 66]. Sedimentation processes are commonly used to separate clean water from solid particles forming sediment with two purposes: to recover and reuse the water resource, and to thicken suspensions. In mineral processing of copper the sedimentation is carried out after the flotation process, where the finely divided mineral is mixed with a huge quantity of water. Thickening occurs in large tanks called thickeners, see Figure 1.1, and the main purpose is the recovery of a big part of the water, essential for the economical and environmental sustainability of the industry. Sedimentation in wastewater treatments plants is performed in two sorts of tanks called clarifiers, the primary clarifier and the secondary clarifier or secondary settling tank (SST). An SST has a similar structure as the thickeners used in mining where in the later, the main purpose is to recover clean water and reuse biomass. In both applications the process is called continuous sedimentation, because there is a continuous feed flow to the vessel, and clean water and sediment are also removed continuously.

The applications of this work focuses on the sedimentation process of small mono-sized solid particles dispersed in a fluid settling to the bottom by gravitational or centrifugal force, and part of it is dedicated to the study the reactive settling. The aim is to study the batch and continuous sedimentation problem under different

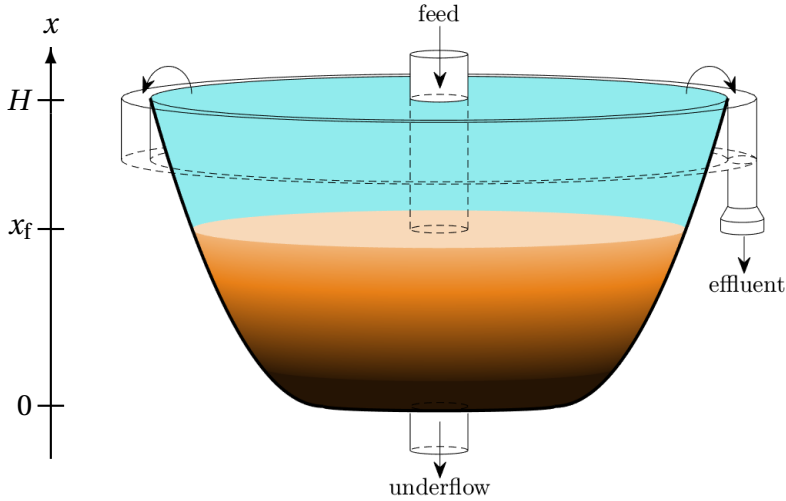


Figure 1.1: Illustration of a secondary settling tank (SST), the height x pointing upward is displayed to the left of the SST showing the bottom $x = 0$, the feed level $x = x_f$ and the top $x = H$ of the vessel.

vessel geometries. The main application is the simulation of the SST in wastewater treatment plants. Numerical simulations of the SST can be used to test different operational conditions, get an approximation of the solid concentration profile inside the vessel, the quantity of clean water recovered and the concentration of the underflow with respect time, and predict the possibility of overflows and unfavorable conditions.

1.2 Motivation for modeling

The sedimentation processes studied here represent a rich problem class from both a physical and mathematical point of view. From a physical point of view, the goal is to find a model that accurately describes the phenomenon and the constitutive relations between variables. From a macroscopic approach the process can be modeled using the theory of continuum mechanics. From this theory, models expressed by partial differential equations (PDEs) can be derived considering the physical quantities and constitutive relations involved. This approach is opposed, for instance, to particle-based descriptions. The main model in this work is a quasi-one-dimensional approximation of a more general one in several dimensions. Modeled by a single PDE, the unknown solid volume fraction ϕ as a function of the height $x \in \mathbb{R}$ and time

$t > 0$ is described by

$$\partial_t(A(x)\phi) - \partial_x(Q(x, t)\phi + \gamma(x)A(x)f(\phi)) = \partial_x(\gamma(x)A(x)a(\phi)\partial_x\phi) + s_f(x, t), \quad (1.1)$$

where the vessel is located between $x = 0$ (bottom) and $x = H$ (top), here $x < 0$ and $x > H$ represent the pipes (outside the vessel), see Figure 1.1, A represents the cross-sectional area as a function of x , f and a are non-linear functions of the unknown ϕ , Q is the volumetric flow, discontinuous at one point of x (the feed inlet), and varies with respect to t , γ is the indicator function which is $\gamma(x) = 1$ if $x \in [0, H]$ and $\gamma(x) = 0$ otherwise, and s_f is a source term singular in x . The main assumption of this model is that the solid volume fraction is a function of height and time only. This model can be used for both, batch and continuous sedimentation, and is presented in detail in Chapter 2. Equation (1.1) has ingredients that make it difficult to analyze. Since Q is discontinuous and f is non-linear, (1.1) has a non-linear discontinuous flux. Furthermore, the function a is zero for an interval of values of ϕ , hence (1.1) is a second-order parabolic strongly degenerate PDE.

The analysis of this model from a mathematical point of view gives rise to various challenges that can be studied separately as independent problems. One of the problems connected to this type of PDEs is the study of existence and uniqueness of solutions, which is related to the search of so-called *entropy solutions*, or physically relevant solutions. Also, the qualitative study of solutions of (1.1) is of interest in, for example, operational control, see [40, 41, 42, 44] for the case of constant cross-sectional area function. Another branch of study is the inverse problem to identify the constitutive functions f and a , which is needed for calibration of the model. On the numerical approximation of solutions, there are several aspects to consider. In the search of reliable numerical methods, it is important to investigate convergence, stability and consistency, and to study orders of convergence, error bounds and efficiency, among others.

1.3 Research questions

The formulation of the mathematical problems treated in this thesis come from physical processes, which are difficult to anticipate and control because of nonlinearities. These physical processes are: Continuous and batch sedimentation with reactions in vessels with varying cross-sectional area; separation by centrifugation; wastewater treatment in sequencing batch reactors. Some of the basic questions related to the construction of the mathematical models are:

- i) How general would the considerations be for the model in terms of number of variables involved and approximations of the reality made?

- ii) What are the physical laws that govern the process? Which constitutive assumptions are needed to be imposed?

Physical laws can be written in terms of nonlinear PDEs, which give rise to general and mathematical research questions:

- iii) How should the initial PDEs obtained from physical laws be reformulated to include suitable constitutive relationships and form a well-posed problem?
- iv) Can one construct a numerical method that gives reliable simulations, which do not take too long to simulate? Do the numerical solutions approximate those of the PDEs? Are discontinuities resolved correctly? Are the simulated concentrations non-negative and the volume fractions between zero and one?
- v) How does one determine the constitutive functions in the PDE? Using data from a large plant or performing tailored experiments in a laboratory? Is it possible to construct new more efficient identification methods than the traditional ones by utilizing the knowledge of the PDE solution?

To answer the latter question and the one under iii) “Are discontinuities resolved correctly by a numerical method?”, further knowledge of the PDE solutions are needed. This leads to the following research questions:

- vi) Is it possible to construct solutions accurately? What are the main structures of the qualitatively different solutions?
- vii) When new simulation and identification methods have been obtained, how do they perform with real data and do they compare to the existing ones?

This thesis means a contribution to the answers of these questions.

1.4 Previous works

One of the first models for sedimentation processes of ideal suspensions was done by Steinour in 1944 [100, 101, 102]. In his work, he introduced a model for the one-dimensional batch sedimentation under the assumption that the velocity of the particles depends only on the local solid volume fraction. Kynch in 1952 [84] showed that the idealized problem in cylindrical vessels can be modeled by a single nonlinear conservation law, and built the solution of the problem by using the method

of characteristics. One of the extensions of Kynch's model to continuous sedimentation was done by Petty in 1975 [92]. In that work he constructed solutions by using the method of characteristics, besides, he analyzed the possible steady state solutions and boundary concentrations.

In 1990, Bustos, Concha and Paiva [27] treated continuous sedimentation as a control problem by an initial boundary value problem. Their model equation neither included the effective solid stress function nor any source term. They built solutions of their problem by subdividing the regions of smoothness and identifying lines of continuity and discontinuity. The main result is the proof that the solution satisfies the Kružkov-type entropy condition. In the same year, Bustos, Concha and Wendland [26] continued exploring the continuous sedimentation problem given in [27] by constructing the corresponding global weak solutions and studying control operations. Bustos and Concha in 1992 [24] showed that in the continuous sedimentation of ideal suspensions the values assumed by the concentration at the boundaries are more restricted than those established by Petty [92]. Gimse and Risebro in 1992 [68] solved a Cauchy problem arising in oil reservoir simulations. The PDE model has a similarity to that for models of continuous sedimentation: the flux function may have discontinuities in the space variable.

One of the first models in one-dimensional sedimentation in vessels with varying cross-sectional area was presented by Chancelier, De Lara and Pacard in 1994 [29], where a complete description of the continuous sedimentation model is given. The model includes a discontinuous flux and singular source term, and the cross-sectional area is added as a weight function to the PDE. Concerning well-posedness (existence and uniqueness), they smoothed the spatial discontinuities and referred to classical results. Furthermore, they also presented an extension of the model to include two types of particles.

Diehl in 1995 [36] elaborated a theoretical framework for non-linear conservation laws with discontinuous flux and singular source term. That work included a uniqueness result based on the so-called condition Γ , which represents a generalization of the classical entropy condition for scalar conservation laws. He also applied this to the problem of continuous sedimentation [37]. Later in 1996 [51], the same author showed that the condition Γ is equivalent to the so-called viscous profile entropy condition. Jeppsson and Diehl in 1996 [78] compared two numerical methods in the simulation of the one-dimensional sedimentation process in cylindrical SSTs and without compression. The first one was based on Godunov's numerical flux and the second on the method by Takács et al. [103]. They concluded that the solutions obtained with the first method are realistic and seemed to converge to the entropic solution unlike the method of Takács which is defined only for 10 fixed layers. A one-dimensional model of continuous sedimentation without compression effect but

including varying cross-sectional area was presented by Diehl in 1997 [38]. In that work a complete description of the steady-state solutions of continuous sedimentation is given. The model has a similar structure as the one presented by Chancelier et al. in [29], and the results obtained can be considered as an extension of [29] for the mono-sized sedimentation case.

Bürger and Wendland in 1998 [21, 22] presented a comprehensive study on entropy solutions of the strongly degenerate parabolic equation with continuous flux modeling sedimentation as an initial-boundary value problem for the thickening zone ($0 < x < x_f$). A contribution about the phenomenological foundation and mathematical theory of sedimentation was published in a book by Bustos and colleagues in 1999 [25].

In 2000, many remarkable contributions to improve the mathematical modelling of batch and continuous sedimentation processes were made [13, 14, 23, 39, 56, 70]. Evje and Karlsen in [56] delved into the entropy solutions of a class of strongly degenerate PDE, which one particular application is the settling and consolidation of suspensions. They also proposed a finite-difference numerical scheme and proved monotonicity and convergence to the entropy solution. Bürger, Evje and Karlsen in [13] studied the quasilinear strongly degenerate parabolic equation with a discontinuous diffusion coefficient arising in mathematical modeling of sedimentation consolidation processes. The same authors together with Lie proposed a conservative numerical scheme satisfying a discrete entropy principle for the simulation of sedimentation processes [14]. The work by Diehl in [39] demonstrated the impact of a converging cross-sectional area on the concentrations at the bottom for incompressible suspensions. He also showed the special treatment needed to define proper boundary conditions satisfying a generalized entropy condition. A detailed derivation of a multi-dimensional model for batch sedimentation is presented by Bürger, Wendland and Concha in [23]. They derived a constitutive relation between the solid-fluid relative velocity and the volume fraction of the solids, and obtained a one-dimensional model in the case of vessels with constant cross-sectional area. Gustavsson and Ooppelstrup in [70] studied the batch sedimentation process in two spatial dimensions including a continuous movement of the bottom wall. A function that simulates the irreversibility of the compression effect is included in the model, and the latter is finally described by a system of coupled PDE and solved numerically using a finite volume scheme.

A one-dimensional model and numerical method for batch and continuous sedimentation that considers vessels with non-constant cross-sectional area is proposed by Bürger, Damasceno and Karlsen in 2004 [7]. The model includes the compression effect and the numerical method developed uses the Engquist-Osher numerical flux, see [54]. The method of characteristics is used to determine the solution without com-

pression considering (only) cylindrical and conical vessels. Solutions for different stationary states with several values of underflow concentrations and some of the solutions obtained with the numerical method for the transient case are shown.

In the work by Bürger, Karlsen, Risebro and Towers in 2004 [17] a model for continuous sedimentation in vessels with constant cross-sectional area is analyzed. They present the notion of entropy condition for the continuous sedimentation model based on the Kružkov entropy condition, together with a series of technical lemmas and essential results to prove the uniqueness of the entropy solution in a particular class of discontinuous functions. They defined a numerical method based on the numerical flux of Engquist-Osher and proved its convergence to the entropy solution. On the other hand, Bürger, Karlsen and Towers in 2005 [18] extended the entropy condition given in [17] which for the case of vessels with constant inner cross-sectional area that has different values for the pipes. Two models are defined, one with constant inner cross-sectional area and the other with a general varying cross-sectional area as function of depth. They define a numerical scheme based on finite differences for the first model and prove convergence of the numerical solutions to the BV_t -entropy solution. Furthermore, the stationary case is studied and some stationary solutions under different feed conditions are obtained. An extended notion of the entropy condition and uniqueness results given in [18] was developed by Diehl in 2009 [46].

An upwind scheme is used by Bürger, Coronel and Sepúlveda in 2006 [6] for the numerical approximation of an initial and boundary value problem of a parabolic strongly degenerate PDE that models different types of sedimentation; gravity settling in a closed vessel, centrifugal settling in a rotating tube and a rotating basket centrifuge. They make a change of variable to simplify the analysis and determine a series of bounds needed to show that the method converges to the entropy solution. In addition, some numerical results for different vessels are shown.

To launch a model framework for continuous sedimentation with compression effects to the wastewater treatment community, a model of continuous sedimentation for SSTs with constant cross-sectional area was introduced by Bürger, Diehl and Nopens in 2011 [12]. This model was later called the *Bürger-Diehl model*. This approach considers a spatially discontinuous flux function, a singular source term due the feed inlet, a degenerate term for the compression effect, and also a function that describes the turbulence near the feed inlet produced by the feed inlet mechanism. This thesis is a continuation of the research about the mathematical modeling of sedimentation processes such as the ones presented above.

Other models have been reported by various authors. In [108], the authors present a set of equations to compute the sludge blanket level of batch settling tests in cylin-

dricl and conical vessels, they also validated this approach with experimental data. In [53], the one-dimensional idealized flux theory is compared with two-dimensional simulations obtained from a CFD program. An approach from the kinematic wave theory applied to sedimentation in vessels with cross-sectional area increasing downward can be found in the works by Schneider [98, 99] and Schaflinger [97]. Schaflinger also worked with experiments on the same problem [96]. An interesting construction of analytical solutions of the model of continuous sedimentation without compression was made by Li and Stenstrom in [86].

For a historical perspective and concise review of the contributions to the research in modeling sedimentation processes during the 20th century, see [30, 31]. For an overview of mathematical problems that emerge from the study of sedimentation processes, see [47] and references therein. For a review of computational fluid dynamics modeling SST over the last three decades, see [62].

One of the aspects studied in this thesis is the inverse problem of flux identification. One of the first methods of flux identification was the graphical method discussed by Kynch in 1952 [84]. The method utilized the construction of the solution the partial differential equation to determine the tail of the flux function.

The modeling and simulation of the reactive settling taking place in the SST takes into account the sedimentation process of multiple solid and liquid phases and also the reactions between them. In wastewater treatment plants, the main reactions of the activated sludge occur in the so-called biological reactor, which is often simulated by ordinary differential equations (ODEs) by assuming a completely homogeneous mixture. Attir and Denn in 1978 [2] introduced one of the first models and numerical algorithm for the simulation of activated sludge in the biological reactor. The model was composed of two ODEs, one for the substrate and one for the biomass component. Henze et al. in 1987 [71] introduced one of the most widely used models (in the recent years) for activated sludge, the activated sludge model number one or ASM1. Detailed treatments of the modeling of biological reactors by systems of ODEs are provided in the books [69, 72]. Further studies about different ODE-based models of activated sludge can be found in [91, 65, 60]. Simulation models and control of activated sludge in the biological reactor and SST combining ODEs and PDEs can be found in [50, 49, 48]. The work presented in Paper IX [4] contains one of the first PDE based models for the simulation of the reactive settling produced in the SST in batch condition. Later, in [11] this model was extended to a general multicomponent model for the reactive settling in the SST under continuous operation.

A combination of biological reactions including settling process is carried out in the so-called sequencing batch reactors (SBRs). The modeling and simulation of

SBRs in the literature is often accomplished without PDE-based models. Irvine, Fox and Richter et al. in 1977 [77] described the SBR process and proposed an ODE-based model in balance laws and chemical reaction of the concentration of waste, organisms and oxygen. He incorporates the fill and draw, and aeration rates in his model equations. A time dependent model which incorporates the concentration of particulate organisms, biomass, inert particulate organics, soluble substrate, soluble intermediate product and soluble inert substrate was proposed by Ibrahim and Abasaed in 1995 [74]. Gao, Peng and Wu in 2010 [61] presented a nitrification-denitrification model for the SBR process. The model is mainly based in the time-dependent differential equations for the ammonium and nitrite concentration. In [107] the authors utilize a mathematical model based on four substrates and two biomass components developed earlier in [55] for the simulation of the SBR describing three phases, the anoxic filling, aerobic filling and react phase. In [76] the authors utilize mathematical models of SBR to study the optimal design and operation of the SBRs. Extended models of SBR to the sequencing batch anaerobic reactors can be found in [57, 89]. Other ODE based models for the simulation of SBR process have been studied in [80, 81, 82, 83].

The inverse problem of flux identification has been studied by utilizing a variety of different techniques. A commonly used method of identification in wastewater treatment community is by the fitting of a prescribed functional flux given a sequence of batch experiments in cylinders [33, 35, 75, 87]. In [32], the authors address the flux identification problem by utilizing functional analysis techniques in the minimization of a non-standard cost functional. In [79], a reconstruction of the unknown flux is carried out from the assumption of a convex flux function and that a single shock wave is formed. A least squares technique in functional spaces is utilized in [58]. And in [28], the inverse problem is formulated as an optimal control problem. The line followed in this thesis is focused in the knowledge of the constructed entropy solutions of the direct problem due to the method of characteristics [8, 43]. For further references about flux identification methods see Paper VIII and references therein.

1.5 Overview of the new results of this thesis

In this work, the solutions are constructed and established results for existence and uniqueness are used, and a qualitative description of the solutions for the case of batch sedimentation is given. Furthermore, we solve the inverse problem of the identification of the flux function f , and validate the identification method with experimental information. In addition, numerical methods for the batch and continuous sedimentation are studied. Models of reactive settling, including suitable nu-

numerical schemes are also outputs of this thesis. Proofs of monotonicity and invariant region properties under CFL conditions (mathematical relations between the space and time steps) are included. One of the benefits of having a numerical scheme satisfying an invariant region property is that the approximated solutions will remain in a bounded region where physical quantities are relevant. The monotonicity of the numerical scheme under a CFL condition ensures the stability of the numerical scheme.

Chapter 2

Model equations for sedimentation

The model is based on the continuum mechanics approach of the theory of mixtures. This theory considers the mixture as a superposition of interacting continuous media, in this case the solid particles and fluid, see [25, 52, 106]. Each of these two phases satisfies the conservation of mass and linear momentum PDEs plus boundary and initial conditions.

2.1 Model equations in 3D

Assume that the sedimentation process occurs in a fixed domain $\Omega \subseteq \mathbb{R}^3$ away from sources. Here the domain Ω represents the vessel. We define the volume fraction of solid particles by $\phi := \phi(\mathbf{x}, t)$ which depends on position $\mathbf{x} \in \Omega$ and time $t \in (0, T]$, where $T \in \mathbb{R}^+$ is the end time. The function ϕ is a scalar quantity and represents the fraction of volume occupied by the solid phase immersed in the fluid, and ϕ_{\max} represents the maximum volume fraction. The conservation of mass for the solid and fluid phases is expressed by

$$\partial_t \phi + \nabla \cdot (\phi \mathbf{u}) = 0, \quad (2.1)$$

$$\partial_t (1 - \phi) + \nabla \cdot ((1 - \phi) \mathbf{v}) = 0, \quad (2.2)$$

where $\mathbf{u} := \mathbf{u}(\mathbf{x}, t)$ and $\mathbf{v} := \mathbf{v}(\mathbf{x}, t)$ are the solid and fluid velocity fields, respectively, vectorial quantities. The equations for conservation of momentum for both phases, solid and fluid, are obtained considering gravity, viscous and interaction forces, in-

cluding also pressure gradients. The momentum equations are

$$\rho_s \phi D_t \mathbf{u} = -\nabla p_s + \nabla \cdot \mathbf{T}_s^E - \rho_s \phi g \mathbf{k} + \mathbf{m}, \quad (2.3)$$

$$\rho_f (1 - \phi) D_t \mathbf{v} = -\nabla p_f + \nabla \cdot \mathbf{T}_f^E - \rho_f (1 - \phi) g \mathbf{k} - \mathbf{m}, \quad (2.4)$$

where $p_s := p_s(\mathbf{x}, t)$ and $p_f := p_f(\mathbf{x}, t)$ are the pressures of solid and fluid, respectively, \mathbf{T}_s^E and \mathbf{T}_f^E are the solid and fluid viscous stress tensors, respectively, g is the acceleration of gravity, \mathbf{k} is the upward unit vector and \mathbf{m} is the solid-fluid interaction force per unit volume. The operator $D_t(\cdot)$ denotes material derivative, that for solid and fluid velocity is defined as

$$D_t \mathbf{u} := \partial_t \mathbf{u} + (\mathbf{u} \cdot \nabla) \mathbf{u}, \quad \left(D_t \mathbf{v} := \partial_t \mathbf{v} + (\mathbf{v} \cdot \nabla) \mathbf{v} \right)$$

Under the constitutive assumptions that the viscous stress tensors \mathbf{T}_s^E , \mathbf{T}_f^E and the interaction force \mathbf{m} depend only on ϕ , \mathbf{u} and \mathbf{v} , the PDE system (2.1)–(2.4) has five unknown functions ϕ , \mathbf{u} , \mathbf{v} , p_s and p_f . By components there are nine unknowns and eight equations, i.e. the system is underdetermined, and an extra relation between the unknowns is needed. The multi-dimensional model by Bürger et al. [23] is the fundamental pillar from which the one-dimensional model studied in this work is derived. The authors consider the viscous term with a similar form as in the Navier-Stokes equations for the solid and fluid phase, i.e.

$$\begin{aligned} \mathbf{T}_s^E &= \mathbf{T}_s^E(\phi, \mathbf{u}) := \mu_s(\phi) (2\boldsymbol{\varepsilon}(\mathbf{u}) + \eta(\phi) (\nabla \cdot \mathbf{u}) \mathbf{I}), \\ \mathbf{T}_f^E &= \mathbf{T}_f^E(\phi, \mathbf{v}) := \mu_f(\phi) (2\boldsymbol{\varepsilon}(\mathbf{v}) + \eta(\phi) (\nabla \cdot \mathbf{v}) \mathbf{I}), \end{aligned}$$

where $\boldsymbol{\varepsilon}(\cdot) = (1/2)(\nabla(\cdot) + \nabla(\cdot)^T)$, the symmetric part of the gradient operator on a vector, \mathbf{I} is the identity matrix, μ_s and μ_f are the viscosity functions for the fluid and solid phase, respectively, and η is a function of ϕ . They also consider that \mathbf{m} is function of ϕ and introduce the relative velocity $\mathbf{v}_r := \mathbf{u} - \mathbf{v}$. Furthermore, they introduce a constitutive relation between the solid and fluid pressures and two new variables, the excess pore pressure p and the extra solid stress $\sigma_e := \sigma_e(\phi)$, reducing the number of unknowns by one. The extra solid stress function satisfies that $\sigma_e'(\phi) = 0$ for $\phi \leq \phi_c$ and $\sigma_e'(\phi) \geq 0$ for $\phi_c < \phi \leq \phi_{\max}$ where $\phi_c \in (0, \phi_{\max}]$ is the critical concentration. After adding the momentum equations and making a dimensional analysis to neglect smaller terms they obtain one of the main results for the relative velocity:

$$\mathbf{v}_r = \mathbf{v}_r(\phi, \nabla \phi) = -\frac{f(\phi)}{\Delta \rho g \phi^2 (1 - \phi)} (\sigma_e'(\phi) \nabla \phi + \Delta \rho g \phi \mathbf{k}), \quad (2.5)$$

where $\Delta \rho = \rho_s - \rho_f$ and $f := f(\phi)$ is a non-linear function that comes from the interaction force \mathbf{m} . This function is called the batch flux density, that in some papers is denoted by f_b or f_{bk} , introduced in [84]. The flux function f can be written in terms of the hindered settling function v_{hs} by $f(\phi) = \phi v_{hs}(\phi)$, and it satisfies:

$f(0) = f(\phi_{\max}) = 0$, $f(\phi) > 0$ for $0 < \phi < \phi_{\max}$, $f'(0) > 0$ and $f'(\phi_{\max}) \leq 0$. The equality (2.5) means that the relative velocity has only functional dependence on ϕ and $\nabla\phi$. Then, grouping terms and introducing a new variable, the volume-average flow velocity of the mixture $\mathbf{q} := \phi\mathbf{u} + (1 - \phi)\mathbf{v} = \mathbf{u} - (1 - \phi)\mathbf{v}_r$, the PDE system (2.1)–(2.4) is reduced to the three PDEs

$$\begin{aligned}\partial_t\phi + \nabla \cdot (\phi\mathbf{q} + \phi(1 - \phi)\mathbf{v}_r) &= 0, \\ \nabla \cdot \mathbf{q} &= 0, \\ \nabla p + \nabla\sigma_e - \nabla \cdot (2\mu(\phi)\boldsymbol{\varepsilon}(\mathbf{q})) &= -\Delta\rho\phi g\mathbf{k} + \nabla \cdot \mathbf{R}(\phi, \mathbf{v}_r),\end{aligned}$$

where the definition of the operator \mathbf{R} involves the gradient and divergence of \mathbf{v}_r and gradient of ϕ . Replacing (2.5), the operator \mathbf{R} can be considered as a function of ϕ and $\nabla\phi$ only, i.e. $\mathbf{R} = \mathbf{R}(\phi, \nabla\phi)$, then the final system is written in the unknowns ϕ , p and \mathbf{q} and given by

$$\partial_t\phi + \nabla \cdot (\phi\mathbf{q} - f(\phi)\mathbf{k}) = \nabla \cdot \left(\frac{f(\phi)\sigma'_e(\phi)}{\Delta\rho g\phi} \nabla\phi \right), \quad (2.6)$$

$$\nabla \cdot \mathbf{q} = 0, \quad (2.7)$$

$$\nabla p + \sigma'_e(\phi)\nabla\phi - \nabla \cdot (2\mu(\phi)\boldsymbol{\varepsilon}(\mathbf{q})) = -\Delta\rho\phi g\mathbf{k} + \nabla \cdot \mathbf{R}(\phi), \quad (2.8)$$

Equations (2.6)–(2.8) define *Model 1* which has been widely used in one-dimensional approximations of sedimentation in vessels with constant cross-sectional area, for example [9, 10, 12, 14, 15, 45, 64], especially for the case of batch sedimentation where the volume-average flow velocity of the mixture is zero, and the problem can be reduced to a one-dimensional second-order parabolic strongly-degenerate non-linear PDE. Also, there are articles dealing with the multi-dimensional case based on this model [19, 20, 22, 93, 94].

The model derived by Gustavsson and Oppelstrup in [70] has the same starting point with the conservation of mass and momentum for the solid and fluid phases. One of the main differences with Model 1 is that the model in [70] is made for the problem of sedimentation that contemplate the possibility to have horizontal movement of the bottom of the vessel. Nevertheless, there are more differences between the two approaches than the inclusion of a horizontal movement. The treatment of the pressures is given in a slightly different way. In [70], the authors have introduced the so-called “memory function” ϕ^* to the definition of the solid pressure, and this term can be compared with the function σ_e with a variable critical concentration. Besides, the fluid stress tensor is neglected. The definition of the interacting force \mathbf{m} is also slightly different in both cases. In the derivation of a reduced PDE system, a dimensional analysis is carried out with the same purpose as in *Model 1*, but in this case this is made separately for both momentum equations, and a different relation

for \mathbf{v}_r was defined. Considering the variables defined in Model 1 this relation is given by

$$\mathbf{v}_r = \frac{f(\phi)}{\Delta\rho g\phi^2(1-\phi)}\nabla p. \quad (2.9)$$

In this case \mathbf{v}_r is function of ϕ and the gradient of the reduced pressure p . We can observe that the relative velocity follows a Darcy-type equation. In [70], this relation is written in terms of the permeability function $K(\phi) = f(\phi)/(\Delta\rho g\phi^2)$. The PDE system derived when following the same idea as in [70] but with the notation and variables defined for Model 1, including the pressure treatment, and without the “memory function”, is

$$\partial_t\phi + \nabla \cdot (\phi\mathbf{u}) = 0, \quad (2.10)$$

$$\nabla \cdot \left(\mathbf{u} - \frac{f(\phi)}{\Delta\rho g\phi^2}\nabla p \right) = 0, \quad (2.11)$$

$$\nabla p + \sigma'_e(\phi)\nabla\phi - \nabla \cdot \mathbf{T}_s^E(\phi, \mathbf{u}) = -\Delta\rho g\phi\mathbf{k}. \quad (2.12)$$

The system (2.10)–(2.12) can be solved for the unknowns ϕ , p and \mathbf{u} , and we will refer to it as *Model 2*. In Model 1 the first two equations (2.6)–(2.7) are decoupled from p . Conversely, in Model 2 this is not satisfied; instead the second equation (2.11) is coupled with the pressure, and the equation can be interpreted as the compressibility of the solid phase. This model is an example of a different approach for the problem, that can be used to simulate the process in the multi-dimensional case. The relations (2.5) and (2.9) are equivalent if $\nabla p = -\sigma'_e(\phi)\nabla\phi - \Delta\rho\phi g\mathbf{k}$, which is in agreement with (2.12) when we neglect \mathbf{T}_s^E . The reasons for the difference in both constitutive relations is the following. To find the constitutive relation (2.5) in [23], \mathbf{T}_s^E and \mathbf{T}_f^E were neglected only in the derivation of \mathbf{v}_r , keeping both terms in the final equation, whereas in [70] just \mathbf{T}_f^E is neglected. If we use the same idea as in [23] and neglect \mathbf{T}_s^E in the dimensionless equation (2.12) only to find a constitutive relation for \mathbf{v}_r and replacing in (2.9), we will obtain (2.5).

Another system of equations can be derived from the set of equations (2.1)–(2.4) in a similar way as Model 2 by neglecting \mathbf{T}_f^E based on a mass-average velocity approach. Defining the mass-average velocity by $\mathbf{v}_m := (\phi\rho_s\mathbf{u} + (1-\phi)\rho_f\mathbf{v})/\rho(\phi)$, where $\rho(\phi) = \rho_s\phi + \rho_f(1-\phi)$, we may rewrite Equation (2.5) as

$$\frac{f(\phi)}{\Delta\rho g\phi^2(1-\phi)}\nabla p = \frac{\rho(\phi)}{\Delta\rho g\phi(1-\phi)}(\mathbf{v}_m - \mathbf{q}).$$

Then, assuming that the solid viscous stress tensors depends on ϕ and \mathbf{v}_m , i.e.,

changing the argument \mathbf{u} by \mathbf{v}_m , $\mathbf{T}_s^E = \mathbf{T}_s^E(\phi, \mathbf{v}_m)$, from (2.10)–(2.12) we obtain

$$\Delta\rho\partial_t\phi + \nabla \cdot (\rho(\phi)\mathbf{v}_m) = 0, \quad (2.13)$$

$$\nabla \cdot \left(\mathbf{v}_m - \frac{v_{hs}(\phi)}{g\rho(\phi)} \nabla p \right) = 0, \quad (2.14)$$

$$\nabla p + \nabla\sigma_e(\phi) - \nabla \cdot \mathbf{T}_s^E(\phi, \mathbf{v}_m) = -\Delta\rho\phi g\mathbf{k}, \quad (2.15)$$

which has the unknowns ϕ , p and velocity field \mathbf{v}_m instead of \mathbf{u} . The main advantage of the system (2.13)–(2.15) is that the second term in (2.14) incorporates a bounded nonlinear term $v_{hs}(\phi)/\rho(\phi)$ instead of $f(\phi)/\phi^2$ which for typical unimodal flux functions [105] tends to infinity when ϕ approaches zero. It seems that this model has not been studied in the literature.

The three models presented are based from full derivations of physical laws and constitutive assumptions. This thesis utilizes one-dimensional approaches of Model 1.

2.2 One-dimensional approach

Models based on one-dimensional approximations of the problem for vessels with constant cross-sectional area have been widely used in applications for continuous and batch sedimentation [5, 34, 35, 104]. Also many simulation software packages are based on this kind of models [59, 63, 67, 95, 109]. The one-dimensional approximation results as a natural assumption since the sedimentation due the gravity force is given essentially in the vertical direction. The aim of this section is to present the derivation of the one-dimensional model of sedimentation in vessels with varying cross-sectional area that is used in the papers that make up this doctoral thesis.

2.2.1 Batch sedimentation with varying cross-sectional area

Let $\Omega \subseteq \mathbb{R}^3$ be the domain, which for batch sedimentation represents the vessel where the sedimentation process occurs, see Figure 2.1. We consider vessels with axisymmetric geometry and circular horizontal cross-section whose area is defined by a non-negative function $A := A(x)$ for $0 \leq x \leq H$, where x is the vertical coordinate (increasing upwards) and H is the height of the vessel. The radius of the horizontal cross-section at the height x is given by $r(x) = (A(x)/\pi)^{1/2}$. The one-dimensional approximation is obtained from the multi-dimensional PDE system (2.1)–(2.2), and using the equations derived in *Model 1*, under the main assumption that the volume fraction is constant at each horizontal cross-section, i.e. $\phi := \phi(x, t)$ for $0 \leq x \leq H$, and that wall effects are negligible. Then the gradient of ϕ (also $1 - \phi$) varies only

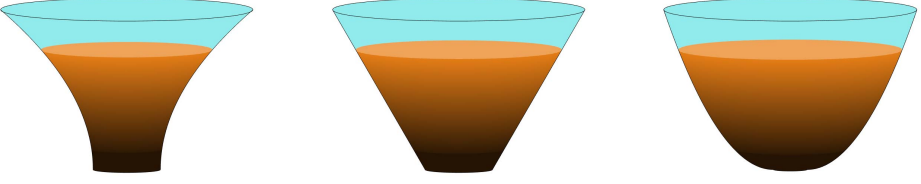


Figure 2.1: Batch sedimentation in three different types of vessels with downward decreasing cross-sectional area.

with respect to x and t . The batch sedimentation is given in closed vessels and can be identified by the absence of in- and outflows. Then the natural boundary conditions for the solid and fluid velocities are $\mathbf{u} \cdot \mathbf{n} = 0$ and $\mathbf{v} \cdot \mathbf{n} = 0$ for \mathbf{n} the outward-pointing normal of $\partial\Omega$, the boundary of Ω . Let $0 \leq x_1 < x_2 \leq H$ and the sub-domain $\tilde{\Omega} := \{\mathbf{x} \in \Omega : x_1 \leq x \leq x_2\}$. Integrating (2.1) over $\tilde{\Omega}$, we get from the first term

$$\int_{\tilde{\Omega}} (\partial_t \phi) \, d\mathbf{x} = \partial_t \int_{\tilde{\Omega}} \phi \, d\mathbf{x} = \partial_t \int_{x_1}^{x_2} A(x) \phi(x, t) \, dx = \int_{x_1}^{x_2} \partial_t (A(x) \phi(x, t)) \, dx. \quad (2.16)$$

The divergence theorem for the second term over the boundary $\partial\tilde{\Omega} = S_1 \cup S_2 \cup S_\partial$, where $S_1 := \{\mathbf{x} \in \partial\tilde{\Omega} : x = x_1\}$, $S_2 := \{\mathbf{x} \in \partial\tilde{\Omega} : x = x_2\}$ and $S_\partial := \partial\Omega \cap \partial\tilde{\Omega}$, implies

$$\begin{aligned} \int_{\tilde{\Omega}} \nabla \cdot (\phi \mathbf{u}) \, d\mathbf{x} &= \int_{S_1} (\phi \mathbf{u}) \cdot (-\mathbf{k}) \, dS + \int_{S_2} (\phi \mathbf{u}) \cdot \mathbf{k} \, dS + \int_{S_\partial} (\phi \mathbf{u}) \cdot \mathbf{n} \, dS \\ &= \phi(x_2, t) \int_{S_2} \mathbf{u} \cdot \mathbf{k} \, dS - \phi(x_1, t) \int_{S_1} \mathbf{u} \cdot \mathbf{k} \, dS. \end{aligned}$$

where \mathbf{k} is the upward unit vector as in Section 2.1. Assuming there is no angular variation, and using cylindrical coordinates for the surface integrals, we have

$$\int_{\tilde{\Omega}} \nabla \cdot (\phi \mathbf{u}) \, d\mathbf{x} = \phi(x_2, t) \int_0^{r(x_2)} 2\pi \mathbf{u} \cdot \mathbf{k} r \, dr - \phi(x_1, t) \int_0^{r(x_1)} 2\pi \mathbf{u} \cdot \mathbf{k} r \, dr. \quad (2.17)$$

In the integrals on the right-hand side \mathbf{u} is considered in cylindrical coordinates. We define the horizontal-average solid velocity

$$\bar{u}(x, t) = \frac{1}{A(x)} \int_0^{r(x)} 2\pi \mathbf{u} \cdot \mathbf{k} r \, dr,$$

which is a scalar quantity that depends only on the spatial coordinate x and time t . Replacing \bar{u} in the equality (2.17) and using the fundamental theorem of calculus, we get

$$\int_{\tilde{\Omega}} \nabla \cdot (\phi \mathbf{u}) \, d\mathbf{x} = \int_{x_1}^{x_2} \partial_x (\phi(x, t) \bar{u}(x, t) A(x)) \, dx. \quad (2.18)$$

Since in both equalities (2.16) and (2.18) the values of x_1 and x_2 were chosen arbitrary, from Equation (2.1) we obtain

$$\partial_t(A(x)\phi) + \partial_x(A(x)\phi\bar{u}) = 0, \quad (2.19)$$

where the arguments of the unknowns ϕ and \bar{u} were omitted only for clarity. The derivation of the one-dimensional version of the conservation of mass for the fluid phase can be made in a similar way using Equation (2.2) and defining \bar{v} by replacing \mathbf{v} instead of \mathbf{u} in the definition of \bar{u} . The one-dimensional version of (2.2) is given by

$$\partial_t(A(x)(1-\phi)) + \partial_x(A(x)(1-\phi)\bar{v}) = 0. \quad (2.20)$$

Using the definition of the horizontal-average velocities \bar{u} and \bar{v} we can define the relative horizontal-average velocity by

$$\bar{v}_r(x, t) := \bar{u}(x, t) - \bar{v}(x, t) = \frac{1}{A(x)} \int_0^{r(x)} 2\pi \mathbf{v}_r \cdot \mathbf{k} r \, dr.$$

Replacing the constitutive relation (2.5) along with the fact that $\nabla\phi = \partial_x\phi\mathbf{k}$, we obtain the one-dimensional constitutive relation

$$\begin{aligned} \bar{v}_r &= \frac{1}{A(x)} \int_0^{r(x)} 2\pi \left(-\frac{f(\phi)}{\Delta\rho g\phi^2(1-\phi)} (\sigma'_e(\phi)\partial_x\phi + \Delta\rho g\phi) \mathbf{k} \right) \cdot \mathbf{k} r \, dr \\ &= -\frac{f(\phi)}{\Delta\rho g\phi^2(1-\phi)} (\sigma'_e(\phi)\partial_x\phi + \Delta\rho g\phi). \end{aligned}$$

Defining

$$\bar{q}(x, t) := \phi\bar{u}(x, t) + (1-\phi)\bar{v}(x, t) = \frac{1}{A(x)} \int_0^{r(x)} 2\pi \mathbf{q} \cdot \mathbf{k} r \, dr,$$

and adding the one-dimensional equations (2.19) and (2.20) we get the one-dimensional approximation of (2.7), $\partial_x(A(x)\bar{q}) = 0$, which implies $A(x)\bar{q}(x, t) = Q(t)$, for Q a function of the time t . Considering that in batch sedimentation the boundary conditions are given by zero flux, $\mathbf{q} \cdot \mathbf{k} = 0$ at the top and $\mathbf{q} \cdot (-\mathbf{k}) = 0$ at the bottom, then replacing this in the definition $\bar{q}(0, t) = \bar{q}(H, t) = 0$, we conclude that $A(x)\bar{q}(x, t) = 0$. Using the relation $\phi\bar{u} = \phi(1-\phi)\bar{v}_r + \phi\bar{q}$, and $\bar{q} = 0$ we obtain the main one-dimensional equation

$$\partial_t(A(x)\phi) - \partial_x(A(x)f(\phi)) = \partial_x \left(\frac{A(x)f(\phi)\sigma'_e(\phi)}{\Delta\rho g\phi} \partial_x\phi \right). \quad (2.21)$$

From the zero-flux boundary conditions at the top $x = H$ we get $\mathbf{u} \cdot \mathbf{k} = \mathbf{v} \cdot \mathbf{k} = 0$, and at the bottom $x = 0$ we have $\mathbf{u} \cdot (-\mathbf{k}) = \mathbf{v} \cdot (-\mathbf{k}) = 0$. These conditions imply that

$\mathbf{v}_r \cdot \mathbf{k} = 0$ at the top and $\mathbf{v}_r \cdot (-\mathbf{k}) = 0$ at the bottom, then $\bar{v}_r(0, t) = \bar{v}_r(H, t) = 0$ and the boundary conditions are given by

$$-f(\phi(x, t)) - a(\phi(x, t))\partial_x(\phi(x, t))|_{x=0, H} = 0.$$

These follow from the zero flux boundary condition and condition Γ , see [37, Section 5]. For $\sigma_e \equiv 0$, since the flux function is assumed to be zero only for $\phi = 0$ and $\phi = \phi_{\max}$, the natural boundary conditions are

$$\phi(0^-, t) = \phi_{\max}, \quad \phi(H^+, t) = 0, \quad t \geq 0.$$

Then (2.21) plus the above boundary conditions and an initial condition $\phi(x, 0) = \phi_0(x)$ can be solved for the unknown $\phi = \phi(x, t)$. Observe that since the equations are decoupled from the pressure in the multi-dimensional model, in this one-dimensional case it is not needed to solve (2.21), and then we need not to solve the momentum equation. On the right hand side of (2.21) the function

$$a(\phi) = \frac{f(\phi)\sigma'_e(\phi)}{\Delta\rho g\phi}$$

is related to the compression of the solid particles, in some applications called d_{comp} , [10, 12].

2.2.2 Continuous sedimentation

The extended one-dimensional model for continuous sedimentation has to manage the inclusion of a feed inlet located at some point $0 < x_f < H$ and outward volumetric flows, the effluent at the top and underflow at the bottom of the vessel. The vessel is divided into two regions, the clarification zone, above the feed inlet and the thickening zone, below the feed inlet, see Figure 2.2. Furthermore, the domain in this case is $\Omega = \mathbb{R}$, which implies also the extension of the cross-sectional area function to the pipes by, for example, $A(x) = A(H)$ for $x > H$ and $A(x) = A(0)$ for $x < 0$, [38]. It is also assumed that hindered settling occurs only inside the vessel, i.e. the batch flux f is zero outside the vessel, for $x < 0$ or $x > H$. The feed inlet is added into the equation through a singular source term that involves the Dirac distribution, the in- and out-flows are included in the function Q , which in this case is not zero and depends also on x , and has a discontinuity in the feed inlet position $x = x_f$. The PDE modeling the process is given by

$$\partial_t(A(x)\phi) - \partial_x(Q(x, t)\phi + \gamma(x)A(x)f(\phi)) = \partial_x(\gamma(x)A(x)a(\phi)\partial_x\phi) + \delta_{x_f}(x)s(t) \quad (2.22)$$

where δ_{x_f} is the x_f -translation of the Dirac distribution δ , $s(t)$ is the mass entering the vessel per time unit, and

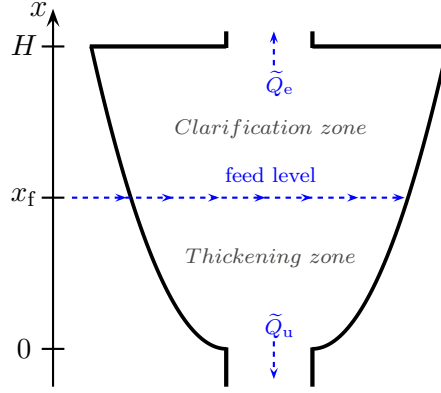


Figure 2.2: Vertical cross-section of the vessel including pipes for the continuous sedimentation process.

$$Q(x, t) = \begin{cases} Q_e(t), & \text{for } x > x_f, \\ Q_u(t), & \text{for } x < x_f, \end{cases} \quad \gamma(x) = \begin{cases} 1, & \text{for } 0 \leq x \leq H, \\ 0, & \text{for } x < 0 \text{ or } x > H. \end{cases}$$

Here the volumetric flows (volume per time unit) Q_e and Q_u are the flow up and down, respectively. In many publications of continuous sedimentation, as in those cited above, also in Paper II, the spatial coordinate is depth instead of height. It is also possible to add a function modeling the dispersion effect produced by the feed inlet mechanism in the same way as in [12]. If $d_{\text{disp}} = d_{\text{disp}}(x)$ is the dispersion function modeling mixing due to the feed inlet, such that $d_{\text{disp}}(x) = 0$ for $x \leq 0$ and $x \geq H$, then this is included in the model equation (2.22) by adding $\partial_x (A(x)d_{\text{disp}}(x)\partial_x \phi)$ on the right-hand side. Similar models can be found in [7, 16, 18, 29, 38].

Chapter 3

Overview and main results of the papers

The purpose of this chapter is to present a compendium of the results obtained in the papers of this thesis, they are divided depending on the topic and contribution made.

The first section of this chapter contains the papers related to theoretical studies of entropy solutions and the inverse problem of flux identification. The second section is about the results obtained from the numerical simulation of the PDEs for the models sedimentation processes, and the third section is about the application of the theoretical results to specific problems in the applied sciences.

3.1 Exact solutions and inverse problem

In the first contribution, Paper I, batch sedimentation of an ideal suspension in a vessel with variable cross-sectional area is modeled by

$$\frac{\partial}{\partial t} (A(x)\phi) - \frac{\partial}{\partial x} (A(x)f(\phi)) = 0, \quad \text{for } x \in (0, 1), t > 0, \quad (3.1)$$

$$\phi(x, 0) = \phi_0, \quad \text{for } x \in (0, 1), \quad (3.2)$$

$$\phi(0^+, t) = 1, \quad \phi(1^-, t) = 0, \quad \text{for } t > 0, \quad (3.3)$$

where ϕ is the local solids volume fraction, A is the cross-sectional area function, f is the flux function, and ϕ_0 is the initial volume fraction (constant). Equation (3.1) is obtained by setting $\sigma_e = 0$ in (2.21), see Chapter 2. The flux f belongs to the set of

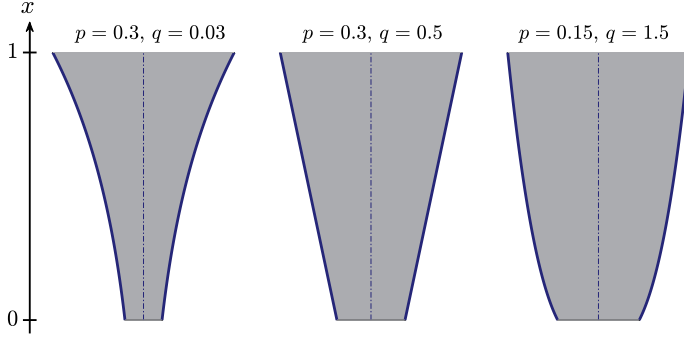


Figure 3.1: Vertical cut of three vessel geometries generated by the cross-sectional area A given by (3.4).

$C^2[0, 1]$ positive unimodal functions, such that $f(0) = f(1) = 0$, and it has not more than one inflection point $\phi_{\text{infl}} > 0$. The point of maximum of f is denoted by $\hat{\phi} \in (0, 1)$. The flux also needs to satisfy that $f''(\phi) < 0$ for $\phi \in (0, \hat{\phi})$. An example of such a flux function is

$$f(\phi) = \phi(e^{-r_V\phi} - e^{-r_V}), \quad \text{for a fixed parameter } r_V > 0.$$

The cross-sectional area function used is given by

$$A(x) = \left(\frac{p + qx}{p + q} \right)^{1/q}, \quad (3.4)$$

with $p, q \neq 0$ two independent parameters. This type of cross-sectional area function includes a wide spectrum of vessel geometries, for example, the truncated cones, see Figure 3.1.

It is well known from the theory of hyperbolic PDEs that the uniqueness of solutions of equations such as (3.1) is not always satisfied [73, 85]. For that reason the concept of *entropic solution* is introduced, which in simple terms means a physically relevant solution. Furthermore, due to the possibility of the existence of solutions with discontinuities, the entropy solutions sought must satisfy jump and entropy conditions.

Apart from studying the existence and uniqueness of entropy solutions, there are a couple of interesting questions regarding regularity and behavior of the solution. Some of them are: Is there a finite number of discontinuities in the solution? Do the discontinuities intersect each other and when? How many regions of smooth solution in the xt -plane are there? This paper has answered all these questions. The entropy solutions were constructed, which were described in detail showing that there exist at most two discontinuities, the upper discontinuity $h := h(t)$ and the bottom

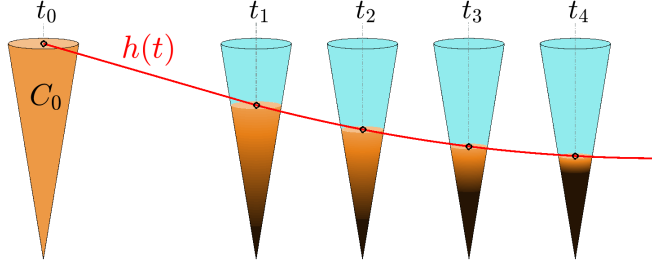


Figure 3.2: Illustration of a batch sedimentation test in a conical vessel. The test starts with homogeneous concentration $C_0 = \rho_s \phi_0$ at t_0 and the settling process is shown for the times $t_1, t_2, t_3,$ and t_4 together with the solid-liquid interface h in red.

discontinuity $b := b(t)$, that may or may not intersect, see Paper I, Figure 3. The solutions were classified into three types of solutions depending on ϕ_0 . The construction of the entropy solutions was based on the method of characteristics, and a set of equations for the discontinuities and solution ϕ was obtained. Uniqueness of the constructed solutions was guaranteed by [90].

The second contribution is Paper II. The upper discontinuity $x = h(t)$, also called the sludge blanket or sediment level, is usually seen in reality and measurable. Figure 3.2 shows a batch test in a conical vessel and the solid-liquid interface trajectory $h := h(t)$. Paper II addresses the inverse problem of flux identification related to the problem (3.1)–(3.3) when $h(t)$ is known. The flux function f satisfies the same assumptions as in Paper I, and the cross-sectional area is given by (3.4) but now with $p \geq 0$ and $q > 0$. Note that in comparison with Paper I, $p = 0$ is included and in this case $A(0) = 0$, hence Equation (3.1) has a singular coefficient. The inverse problem is formulated as follows:

Given $\phi_0 > 0$ and the interface trajectory $[t_{\text{start}}, t_{\text{end}}] \ni t \mapsto h(t)$ (the sludge blanket level), find the portion of the flux function $\phi \rightarrow f(\phi)$ corresponding to the interval of ϕ -values adjacent to that trajectory.

The solution of this problem is based in the knowledge of the construction of the entropy solutions of (3.1). For the inverse problem when $p = 0$ and $q > 0$, the analysis and construction of the entropy solutions were included.

Since the flux function f depends on the application, the solution of the inverse problem can be used to create a method for the calibration of the model (3.1)–(3.3). Some of the questions of interest to be answered by Paper II are about the existence of solutions, the type of solutions (implicit, explicit or parametric), the size of the

portion of flux that can be identified, and how to apply the solution to handle real data from experiments.

The solution developed is built principally from the ODEs derived from the construction of the entropy solutions in Paper I and for the case $p = 0$ ($q > 0$). The parametric solution (with $p \geq 0$ and $q > 0$) found is

$$\begin{pmatrix} \phi \\ f(\phi) \end{pmatrix} = \frac{\phi_0(p+q)^{1+1/q}}{(p+qh(t))^{1/q}(p+q(h(t)-th'(t)))} \begin{pmatrix} 1 \\ -h'(t) \end{pmatrix}, \quad 0 \leq t \leq t_{2.5}, \quad (3.5)$$

and an explicit formula is given by

$$f(\phi) = -\phi h'(\sigma^{-1}((\phi_0/\phi)(p+q)^{1+1/q})),$$

where $\sigma(t) := s(t) - qts'(t)/(q+1)$, $s(t) = (p+qh(t))^{1/q+1}$ and $t_{2.5}$ is the time point where h' has a discontinuity. The length of the ϕ -interval of the identified flux depends mainly on $t_{2.5}$, which is difficult to obtain without solving ODEs and using f (which is unknown in the inverse problem). When p tends to zero, the ϕ -interval increases in length, see Paper II, Figure 3. Furthermore, the entropy solution when $p = 0$ and $q > 0$ (for ϕ_0 sufficiently big) does not contain any bottom discontinuity and $t_{2.5}$ coincides with the steady state starting point. Hence, the conclusion reached is that in the case when $p = 0$ and $q > 0$, the flux function can be identified in the maximal interval $[\phi_0, 1]$. The best solution is then given in the case of a vessel with downward-decreasing cross-sectional area with vertex at $x = 0$. An underlying result is that the geometry of the vessel has an unexpected positive influence on the solution of the inverse problem. This method of identification represents a significant advance compared to traditional methods of flux identification. Finally, examples of the identified flux with synthetic data and with published experimental data are presented, see Paper II, Figures 5 to 7.

The third contribution, Paper III, explores a different settling process, the centrifugal sedimentation of an ideal suspension in a rotating tube or basket. As in Paper I, this process is modeled by an initial-boundary-value problem for a scalar conservation law with a nonconvex flux function. The sought unknown is the volume fraction of solids $\phi := \phi(r, t)$ as a function of the radial distance $r > 0$ measured from the axis of rotation $r = 0$, and time $t \geq 0$. The initial value is constant (homogeneous concentration) and denoted by ϕ_0 . The model is given by

$$\frac{\partial \phi}{\partial t} + \frac{1}{r^\gamma} \frac{\partial}{\partial r} (f(\phi)\omega^2 r^{1+\gamma}) = 0, \quad \text{for } r \in (r_0, r_1), t > 0, \quad (3.6)$$

$$\phi(r, 0) = \phi_0, \quad \text{for } r \in (r_0, r_1), \quad (3.7)$$

$$\phi(r_0^+, t) = 0, \quad \phi(r_1^-, t) = 1, \quad \text{for } t > 0, \quad (3.8)$$

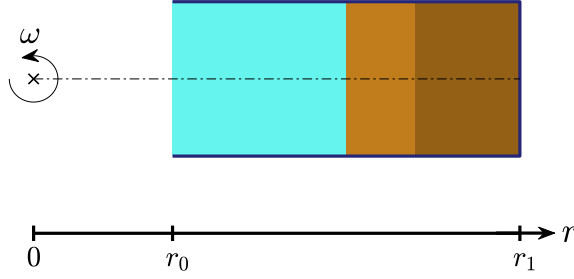


Figure 3.3: Schematic of the centrifugal settling process in a tube of dimensions $0 < r_0 < r_1$ rotating with angular speed ω .

where $0 < r_0 < r_1$ are the vessel coordinates, ω is the constant angular speed of rotation and $\gamma \in \{0, 1\}$ distinguishes between the two types of vessel considered, a rotating tube ($\gamma = 0$) and a cylindrical basket rotating around its axis of symmetry ($\gamma = 1$). Figure (3.3) shows an illustration of the centrifugal settling process. An application of this model is the separation of white blood cells from a blood sample.

The aim of Paper III is to give a full description of the entropy solutions, but also to study the inverse problem of flux identification of (3.6)–(3.8). In a first instance, this article seeks to construct the unique entropy solutions, characterize and give a detailed description of them, and provide a set of equations needed to solve the inverse problem. The same questions from Paper I and Paper II can be formulated for this problem.

In the same way as in Paper I, the entropy and jump conditions are used for the specific PDE (3.6). The method of characteristics is used, and a set of ODEs is obtained to compute the characteristic curves and discontinuities. The entropy condition contains at most two discontinuities $h := h(t)$ (“upper” discontinuity) and $b := b(t)$ (“bottom” discontinuity), see Paper III, Figure 4. The analysis and entropy solutions found have some differences from Paper I. The main difference is that the “bottom discontinuity” b may not merge from the boundary $r = r_1$, and three types of solutions are described depending on the initial value ϕ_0 , the cases are also subdivided depending on the interactions of the discontinuities.

The inverse problem here is defined in the same way as in Paper II (note that the solid-liquid interface is denoted by h in both papers), and the parametric solution is also determined by using the equations provided in the construction of the entropy solutions, and given by

$$\begin{pmatrix} \phi \\ f(\phi) \end{pmatrix} = \phi_0 \left(\frac{r_0}{h(t)} \right)^{1+\gamma} \begin{pmatrix} 1 \\ h'(t) / (\omega^2 h(t)) \end{pmatrix}, \quad 0 \leq t \leq t_i, \quad (3.9)$$

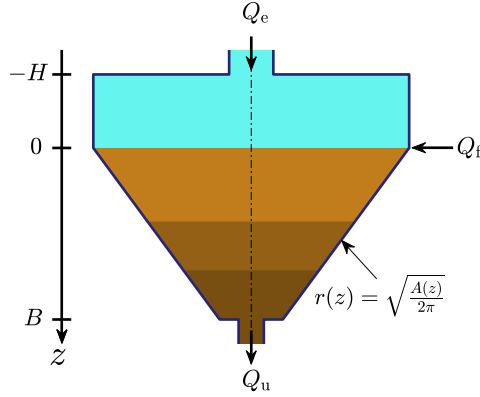


Figure 3.4: Diagram of the vertical cross-section of a settling tank of cross-sectional area function A used in continuous sedimentation. The bulk flows Q_u (underflow), Q_e (effluent) and Q_f (feed) are pointed in the figure. The contour of the vessel (blue) is determined by the radius $r = r(z)$.

where t_i is the time point when h changes its curvature. Furthermore, the following closed formula was found

$$f(\phi) = \frac{\phi h' (h^{-1} (r_0 (\phi_0 / \phi)^{1/(1+\gamma)}))}{\omega^2 r_0 (\phi_0 / \phi)^{1/(1+\gamma)}},$$

where h^{-1} may only be defined implicitly. Conversely to Paper II, the identified flux obtained is to the left of the initial condition ϕ_0 . The formula (3.9) is tested with synthetic data obtained from the numerical approximation of (3.6). For the case of rotating baskets, it can be seen that for big values of ϕ_0 , i.e., ϕ_0 tending to 1, the value of $\phi(t_i)$ tends to zero, and almost the entire flux function can be identified, see Paper III, Figure 10. The pros and cons of this identification method compared with the one developed in Paper II are described in Paper IX.

3.2 Numerical schemes and simulation models

In Paper IV a model for the process of continuous sedimentation in clarifier-thickeners (settlers) with variable cross-sectional area is presented. The PDE describes the concentration of solid particles $C = C(z, t)$, where z is the depth and t time. The spatial domain of the PDE is now the entire real line, and the vessel is considered to be located between $z = -H$ (top) and $z = B$ (bottom), with $H, B > 0$, see Figure 3.4. The model equation can be obtained from (2.22) by setting $x = -z$, $C(z, t) = \rho_s \phi(z, t)$ (ρ_s

the density of solids) and adding a term for the dispersion effect produced by the feed mechanism:

$$\frac{\partial(A(z)C)}{\partial t} + \frac{\partial}{\partial z} (Q(z, t)C + \gamma(z)A(z)f(C)) = \frac{\partial}{\partial z} \left(A(z) \{ \gamma(z)d_{\text{comp}}(C) + d_{\text{disp}}(z, t) \} \frac{\partial C}{\partial z} \right) + s_f(t)\delta(z),$$

where $\gamma(z) = 1$ for $-H \leq z \leq B$ and zero otherwise, the function d_{comp} denotes a in Equation (2.22). The source term is $s_f(t) = Q_f(t)C_f(t)$ with Q_f and C_f the bulk feed flow and feed concentration, respectively, and δ is the dirac distribution.

The main goal and contribution of this work was to extend the Bürger-Diehl settler model in [12] to the case of vessels with varying cross-sectional area. The inclusion of the cross-sectional area function results natural knowing the influences of the vessel geometry in, for example, the inverse problem presented in Paper II.

In the same line as in [12], a numerical scheme based on Godunov's flux and finite differences for the second order derivatives is introduced. The numerical scheme is proved to be monotone under an advantageous CFL condition. The monotonicity implies that the numerical scheme is reliable and the approximated solutions physically relevant. The way how the cross-sectional area function is handled allows conical vessels with a vertex at the bottom to be simulated. Another advantage is that the numerical scheme is given in a method of lines formulation (MOL), this is of special interest for wastewater treatment community, since it is easier to be implemented in ODE solvers. Simulations of continuous sedimentation for various cross-sectional area functions show the influence of the vessel geometry in the concentration profiles and underflow concentrations. Furthermore, batch settling simulations in conical vessels with a vertex at the bottom are also presented, see Paper IV, Figure 5.

The second contribution about numerical schemes and simulation models is Paper V, where the reactive settling process is studied. The unknown solid and liquid phases are composed by multiple components that may react with each other. The solid phase is then given by a vector of concentrations $\mathbf{C} = (C^{(1)}, \dots, C^{(k_c)})$ where some of the components are some type of biological heterotrophic organism. The liquid phase is composed by the vector of substrates $\mathbf{S} = (S^{(1)}, \dots, S^{(k_s)})$ and the concentration of water W . The total solids concentration is denoted by X . These functions depend on the space coordinates z (depth) and time $t > 0$. The system of PDEs

governing this application is given by

$$\frac{\partial(A(z)\mathbf{C})}{\partial t} + \frac{\partial}{\partial z}(A(z)\mathcal{F}_C(z, t, X)\mathbf{C}) = \frac{\partial}{\partial z}\left(A(z)\gamma(z)\frac{\partial D_C(X)}{\partial z}\mathbf{C}\right) + \mathcal{B}_C(\mathbf{C}, \mathbf{S}, z), \quad (3.10)$$

$$\frac{\partial(A(z)\mathbf{S})}{\partial t} + \frac{\partial}{\partial z}(A(z)\mathcal{F}_S(z, t, X)\mathbf{S}) = \frac{\partial}{\partial z}\left(A(z)\gamma(z)\mathcal{D}\frac{\partial \mathbf{S}}{\partial z}\right) + \mathcal{B}_S(\mathbf{C}, \mathbf{S}, z), \quad (3.11)$$

$$X = X(z, t) = C^{(1)}(z, t) + \dots + C^{(k_C)}(z, t), \quad (3.12)$$

where \mathcal{F}_C and \mathcal{F}_S (scalars) are the velocity of the solid components and soluble substrates, respectively, D_C contains the compression function d_{comp} , the matrix \mathcal{D} contains the constants of diffusion for the substrates, and \mathcal{B}_S and \mathcal{B}_C involve the feed and reaction terms of \mathbf{C} and \mathbf{S} , respectively. This model can be seen as an extension of Paper IV to the reactive case. Instead of one single PDE, now there are $k_C + k_S$ equations. Equation (3.10) is influenced by (3.11) through the reaction term in \mathcal{B}_C , conversely, (3.11) depends on \mathbf{C} though its velocity \mathcal{F}_S and function \mathcal{B}_S . Observe that the function \mathcal{F}_S does not depend on \mathbf{S} .

A numerical method based on a combination of upwind approximations that exploits the particular structure of the PDE system is introduced. The semi-discrete numerical scheme is written in method-of-lines formulation, which is a desirable feature when simulating wastewater treatment processes. The monotonicity of the fully-discrete numerical scheme is proved and the main mathematical result is an invariant-region property, which implies that the numerical solutions produced are physically relevant. Numerical simulations for a simplified denitrification model in SSTs (Secondary Settling Tanks) are presented, see Paper V, Figure 5.

The third contribution is Paper VI. That work is about modeling and simulation of sequencing batch reactors (SBRs) applied to the field of wastewater treatment. The PDE model proposed is based on the one presented in Paper V, but there is a moving boundary that varies depending on the bulk flows (in and out). The unknowns are the same as in Paper V, i.e., \mathbf{C} , \mathbf{S} and X as functions of depth z and time t . The model equations are given by

$$\begin{aligned} A(z)\frac{\partial \mathbf{C}}{\partial t} + \frac{\partial}{\partial z}(A(z)\mathcal{F}_C(z, t, X)\mathbf{C}) - \frac{\partial}{\partial z}\left(A(z)\gamma(z, t)\frac{\partial D_C(X)}{\partial z}\mathbf{C}\right) \\ = \delta(z - \bar{z}(t))Q_f(t)\mathbf{C}_f(t) + \gamma(z, t)A(z)\mathbf{R}_C(\mathbf{C}, \mathbf{S}), \end{aligned} \quad (3.13)$$

$$\begin{aligned} A(z)\frac{\partial \mathbf{S}}{\partial t} + \frac{\partial}{\partial z}(A(z)\mathcal{F}_S(z, t, X)\mathbf{S}) \\ = \delta(z - \bar{z}(t))Q_f(t)\mathbf{S}_f + \gamma(z, t)A(z)\mathbf{R}_S(\mathbf{C}, \mathbf{S}), \end{aligned} \quad (3.14)$$

$$X(z, t) = C^{(1)}(z, t) + \dots + C^{(k_C)}(z, t), \quad (3.15)$$

where $\bar{z} := \bar{z}(t)$ is the location of the moving boundary at the time t , $\gamma = \gamma(z, t)$ is the indicator function which equals one if $\bar{z}(t) < z < B$ and zero otherwise, \mathbf{C}_f and

\mathbf{S}_f are the feed concentrations and Q_f is the volumetric feed. The terms $\mathbf{R}_C(\mathbf{C}, \mathbf{S})$ and $\mathbf{R}_S(\mathbf{C}, \mathbf{S})$ are the reaction functions. The rest of the functions are defined as in Paper V. The model covers the operation of an SBR in cycles of consecutive fill, react, settle, draw, and idle stages.

The main question answered by this paper is about how to extend the model in Paper V to simulate SBRs including a moving boundary, and how to handle this in a numerical scheme. Models for SBRs have been developed mainly considering only temporal variations by means of ODEs [57, 74, 76, 89]. As it has been seen in Paper V, the concentrations inside the vessel for a fix time point are not always constant and therefore the neglect of the spatial variations is not desirable. Paper VI contributes to fill the lack of studies that take into account spatial variations of the unknowns and functions. (Observe that in comparison to (3.11), here the diffusion matrix of the soluble substrats \mathcal{D} is not included.)

The location of the moving boundary \bar{z} is determined by the ODE:

$$\bar{z}'(t) = (Q_u(t) - \bar{Q}(t)) / A(\bar{z}(t)),$$

where Q_u is the underflow rate and \bar{Q} is equal to either Q_f , the feed volumetric flow, or Q_e the effluent flow. The upper boundary varies depending on the volumetric flows and cross-sectional area function and hence can be determined before solving (3.13)–(3.15). A suitable monotone numerical scheme that handles the conservation of mass is developed. Simulations of the SBR process with the developed numerical scheme are presented, see Paper VI, Figures 4 and 6.

3.3 Applications and dissemination

The first contribution is Paper VII. That paper consists of the validation of the identification method developed in Paper II. Experiments in conical vessels using real data collected from the wastewater treatment plant in Västerås, Sweden, were performed by a collaborator. The experiments were carried out to measure the descending sludge-supernatant interface (sludge blanket), which is the upper discontinuity h from Paper II. The identification method proposed is the following:

1. Perform a batch-settling test in a vessel such that the suspension fills out a cone with its vertex at the bottom and with the initial homogeneous concentration C_0 . Let H be the height of the suspension surface above the bottom vertex. Collect data points (t_j, h_j) , $j = 1, \dots, N$, along the descending solid-liquid interface.

2. Fit a curve $x = h(t)$ to the data set $\{(t_j, h_j) : j = 1 : 1, \dots, N\}$, for example, with a least-squares method.
3. The estimated portion of the flux function is given by the following parametrization:

$$\begin{cases} C = \frac{C_0 H^3}{(h(t))^2 (h(t) - t h'(t))} \\ f_{\text{par}}(C) = -\frac{C_0 H^3}{(h(t))^2 (h(t) - t h'(t))} h'(t) \end{cases} \quad \text{for } 0 \leq t \leq t_N.$$

This gives the shape of the flux function in the interval $[C_0, C(t_N)]$. To obtain a full flux, the representation in the interval $[0, C_0]$ can be a second-order polynomial p satisfying $p(0) = f_{\text{par}}(0) = 0$, $p(C_0) = f_{\text{par}}(C_0)$ and $p'(C_0) = f'_{\text{par}}(C_0)$ and for the interval $[C(t_N), C_{\text{max}}]$ a straight line can be fitted. The value C_{max} is the maximum concentration of solid particles.

4. An approximate and explicit representation of the flux function can be obtained by a nonlinear fit to the parametric representation f_{par} .

This method is tested with the real data and the identified flux functions are reported. Comparison between the experimental sludge-supernatant interface and the one simulated using the identified fluxes were made, see Paper VII, Figures 3 and 4.

Some of the practical advantages of this method of identification are that no advanced equipment is needed and that with only one experiment a large portion of the flux can be obtained.

The second contribution is Paper VIII. In that article methods of flux identification are reviewed and compared from a theoretical point of view. The methods studied are the ones derived from models of sedimentation described by PDEs with no prescribed formula for the constitutive flux function. A common assumption of models of flux identification is that compression effects are neglected. Five methods of identification are reviewed and compared with synthetic data (from numerical simulations). Among them are the identification methods presented in Paper II and III. Paper VIII contributes to show the advantages of the methods developed in this thesis compared with the old ones from the literature.

Chapter 4

Two-dimensional numerical simulations

This chapter includes non-published material about the simulation of sedimentation processes in two-dimensional domains. This extra material is presented here to show some of the excursions in the multi-dimensional problems made by the author. Part of Section 4.3 was elaborated together with Dr. Ricardo Ruiz-Baier during my stay at University of Oxford, United Kingdom.

4.1 Simplified batch settling

As a first approach, a simplified version of Equation (2.6) is considered. As it was seen in Chapter 2, in the one-dimensional case, the volume average velocity q is zero for batch settling, although in the case of more spatial dimensions this may not be true. In this first attempt the contribution of q to the flux is neglected. Furthermore, setting σ_e to zero, for a two-dimensional domain Ω , Equation (2.6) can be written as

$$\partial_t \phi + \nabla \cdot (f(\phi) \mathbf{k}_\theta) = 0, \quad \mathbf{x} \in \Omega, \quad (4.1)$$

$$f(\phi) \mathbf{k}_\theta \cdot \mathbf{n} = 0, \quad \mathbf{x} \in \partial\Omega, \quad (4.2)$$

$$\phi(\mathbf{x}, 0) = \phi_0, \quad \phi_0 \in (0, 1), \quad (4.3)$$

where $\mathbf{x} = (x, z)$, \mathbf{n} is the normal vector of $\partial\Omega$ and $\mathbf{k}_\theta := (\cos(\theta), \sin(\theta))^T$ is the unit vector in the direction of the force, with $\theta \in [-\pi, \pi]$, this vector incorporates the possibility of having a rotation of the domain. Note that the default case is $\theta = -\pi/2$. Then the vector becomes $\mathbf{k}_{-\pi/2} = -\mathbf{k}$, when the force is pointing in the gravity direction.

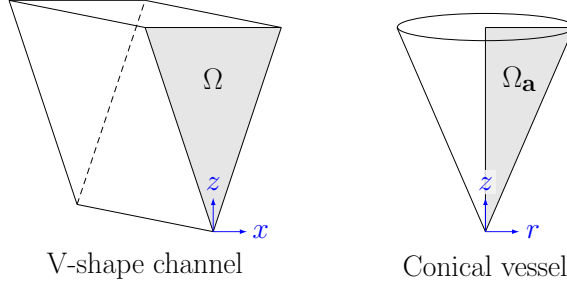


Figure 4.1: Illustration of the domain Ω (left) and the axisymmetrical domain $\Omega_{\mathbf{a}}$ (right).

From Equation (4.1) one can think in the case of domains in \mathbb{R}^3 which are axisymmetric with respect to the z -axis, i.e., domains that are created by the rotation of a two-dimensional set, e.g., $\Omega_{\mathbf{a}} \subseteq \mathbb{R}^2$, where the subscript \mathbf{a} denotes axisymmetry. Figure 4.1 shows the conceptual differences between the two-dimensional domain Ω , vertical cross-section of a V-shaped vessel and $\Omega_{\mathbf{a}}$ whose rotation generates a conical vessel. Under the assumption of axisymmetry of the unknowns (no angular variation), the axisymmetric version of (4.1) in the domain $\Omega_{\mathbf{a}}$ is given by

$$\partial_t \phi + \nabla_{\mathbf{a}} \cdot (f(\phi) \mathbf{k}_{\theta}) = 0, \quad \mathbf{x} \in \Omega_{\mathbf{a}}, \quad (4.4)$$

$$f(\phi) \mathbf{k}_{\theta} \cdot \mathbf{n} = 0, \quad \mathbf{x} \in \partial\Omega_{\mathbf{a}}, \quad (4.5)$$

$$\phi(\mathbf{x}, 0) = \phi_0, \quad \phi_0 \in (0, 1), \quad (4.6)$$

where in this case $\mathbf{x} = (r, z)$, \mathbf{n} is the normal of $\partial\Omega_{\mathbf{a}}$, $r > 0$ is the radius from the center of rotation, and the \mathbf{a} -gradient and \mathbf{a} -divergence operators for a vector field \mathbf{w} in cylindrical coordinates are defined by

$$\nabla_{\mathbf{a}} \mathbf{w} := \begin{pmatrix} \partial_r w_r & \partial_r w_z \\ \partial_z w_r & \partial_z w_z \end{pmatrix}, \quad \nabla_{\mathbf{a}} \cdot \mathbf{w} := \partial_z w_z + \frac{1}{r} \partial_r (r w_r).$$

For the simulations in this chapter, the following unimodal flux function is considered

$$f(\phi) := v_0 \phi (\exp(-r_V \phi) - \exp(-r_V)), \quad \text{with } v_0 = 0.0176 \text{ m/s}, \quad r_V = 4.5. \quad (4.7)$$

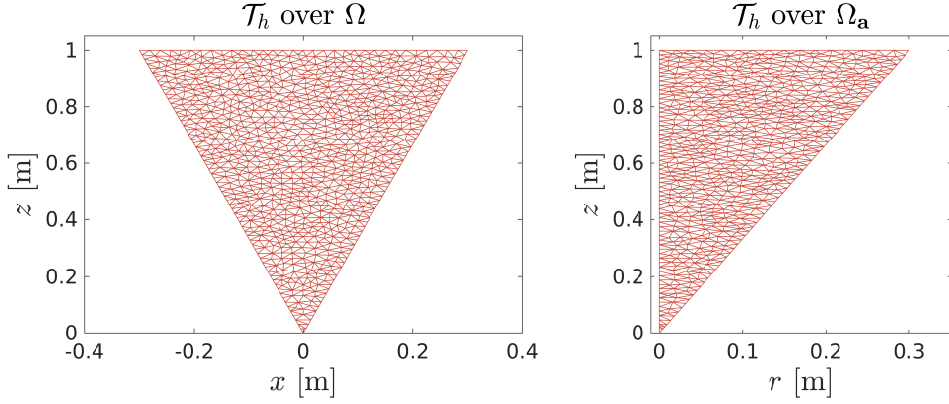


Figure 4.2: Triangulation mesh on Ω and $\Omega_{\mathbf{a}}$.

4.1.1 Numerical scheme

The domain Ω , or possibly $\Omega_{\mathbf{a}}$, is partitioned by a locally regular triangulation \mathcal{T}_h (Delaunay triangulation), on which every triangle $K \in \mathcal{T}_h$ of diameter h_K satisfies:

$$\exists C > 0 : \forall K \in \mathcal{T}_h : \quad Ch_K^2 \leq |K| \leq h_K^2,$$

where $|K|$ is the area of the triangle, C is a constant independent of h , and the mesh parameter h is defined by $h = \max\{h_K : K \in \mathcal{T}_h\}$. Let $\mathcal{N}_h := \{s_j : j = 1, \dots, N\}$ be the set of nodes of the triangles in \mathcal{T}_h , and $\mathcal{E}_h(K)$ the set of edges of a triangle $K \in \mathcal{T}_h$. Furthermore, the triangulation \mathcal{T}_h is considered to be independent of time. Figure 4.2 shows two triangularizations \mathcal{T}_h for the case of a two-dimensional triangular domain Ω , vertical cross-section of a V-shaped vessel, and the triangularization of the half triangle $\Omega_{\mathbf{a}}$ whose rotation generates a conical three-dimensional domain.

In what follows a standard cell-centered finite volume scheme for Equation (4.1) is derived. Integrating Equation (4.1) over a triangle $K_i \in \mathcal{T}_h \in \mathcal{T}_h$ and using the Divergence theorem, we have

$$\int_{K_i} (\partial_t \phi) \, d\mathbf{x} + \int_{K_i} \nabla \cdot (f(\phi) \mathbf{k}_\theta) \, d\mathbf{x} = \partial_t \left(\int_{K_i} \phi \, d\mathbf{x} \right) + \int_{\partial K_i} (f(\phi) \mathbf{k}_\theta) \cdot \mathbf{n} \, ds = 0. \quad (4.8)$$

where in the last integral, \mathbf{n} denotes the normal of ∂K_i , and in what follows \mathbf{n} will denote the normal depending on the domain of integration. Approximating the PDE solution ϕ by its average over K_i

$$\phi_i = \frac{1}{|K_i|} \int_{K_i} \phi \, d\mathbf{x},$$

the integral equation (4.8) can be approximated by the following Finite Volume scheme

$$|K_i| \frac{d\phi_i}{dt} + \int_{\partial K_i} \hat{\mathbf{F}} \cdot \mathbf{n} ds = 0, \quad (4.9)$$

where $\hat{\mathbf{F}}$ denotes the numerical flux at the boundary ∂K_i approximating $f(\phi)\mathbf{k}_\theta$. The computation of $\hat{\mathbf{F}} \cdot \mathbf{n}$ is carried out by Godunov's numerical flux; given two adjacent cells $K_i, K_j \in \mathcal{T}_h$ and the shared edge $e = \partial K_i \cap \partial K_j$ with unit normal \mathbf{n}_e (pointing in the direction from K_i to K_j), the flux at e is given by

$$\hat{\mathbf{F}} \cdot \mathbf{n}_e := \begin{cases} -G(\phi_i, \phi_j) \mathbf{k}_\theta \cdot \mathbf{n}_e & \text{if } \mathbf{k}_\theta \cdot \mathbf{n}_e \geq 0, \\ G(\phi_j, \phi_i) |\mathbf{k}_\theta \cdot \mathbf{n}_e| & \text{if } \mathbf{k}_\theta \cdot \mathbf{n}_e < 0, \end{cases}$$

where $G = G(\phi_i, \phi_j)$ is Godunov's flux between K_i and K_j , which for the unimodal function f can be computed by [1]

$$G(\phi_i, \phi_j) := \min \{ f(\min \{\phi_i, \hat{\phi}\}), f(\max \{\phi_j, \hat{\phi}\}) \}$$

with $\hat{\phi}$ the point of maximum of f . In the case of boundary edges, $e \in \partial\Omega$, the flux is zero. For the time discretization, let Δt be the time step (constant), and $t_n = n\Delta t$, for $n \in \mathbb{N}$, the discrete time points. From now on, the superscript n will denote time evaluation of the time dependent functions at t_n . Approximating the time derivative at (4.9) by forward finite differences, we obtain the fully discrete finite volume approximation of (4.1)

$$|K_i| \frac{\phi_i^{n+1} - \phi_i^n}{\Delta t} + \sum_{e \in \mathcal{E}_h(K_i)} |e| \hat{\mathbf{F}}^n \cdot \mathbf{n}_e = 0, \quad i = 1, \dots, |\mathcal{T}_h|. \quad (4.10)$$

where $|e|$ is the length of the edge e . The upper bound for the time step Δt is given by the CFL condition:

$$\Delta t \leq \frac{1}{C_h \|f'\|_\infty} \quad \text{where} \quad C_h := \max_{K \in \mathcal{T}_h} \left\{ \sum_{e \in \mathcal{E}_h(K)} \frac{|e|}{|K|} \right\}.$$

In the same way as before, one can approximate Equation (4.4) by a finite volume scheme like (4.10), in this case we obtain the fully discrete finite volume approximation

$$\frac{\phi_i^{n+1} - \phi_i^n}{\Delta t} \int_{K_i} r \, d\mathbf{x} + \sum_{e \in \partial K_i} (\hat{\mathbf{F}}^n \cdot \mathbf{n}_e) \int_e r \, ds = 0, \quad i = 1, \dots, |\mathcal{T}_h|. \quad (4.11)$$

In the above formula, the main differences with (4.10) are the integral terms containing r over the triangles and its edges. For a triangle K with vertices $\mathbf{x}_1 = (r_1, z_1)$,

$\mathbf{x}_2 = (r_2, z_2)$ and $\mathbf{x}_3 = (r_3, z_3)$, and edge e between the nodes \mathbf{x}_1 and \mathbf{x}_2 we have

$$\int_K r \, d\mathbf{x} = \begin{vmatrix} r_2 - r_1 & r_3 - r_1 \\ z_2 - z_1 & z_3 - z_1 \end{vmatrix} \left(\frac{r_1}{2} + \frac{r_2 - r_1}{6} + \frac{r_3 - r_1}{6} \right),$$

$$\int_e r \, ds = |e| \frac{(r_1 + r_2)}{2}.$$

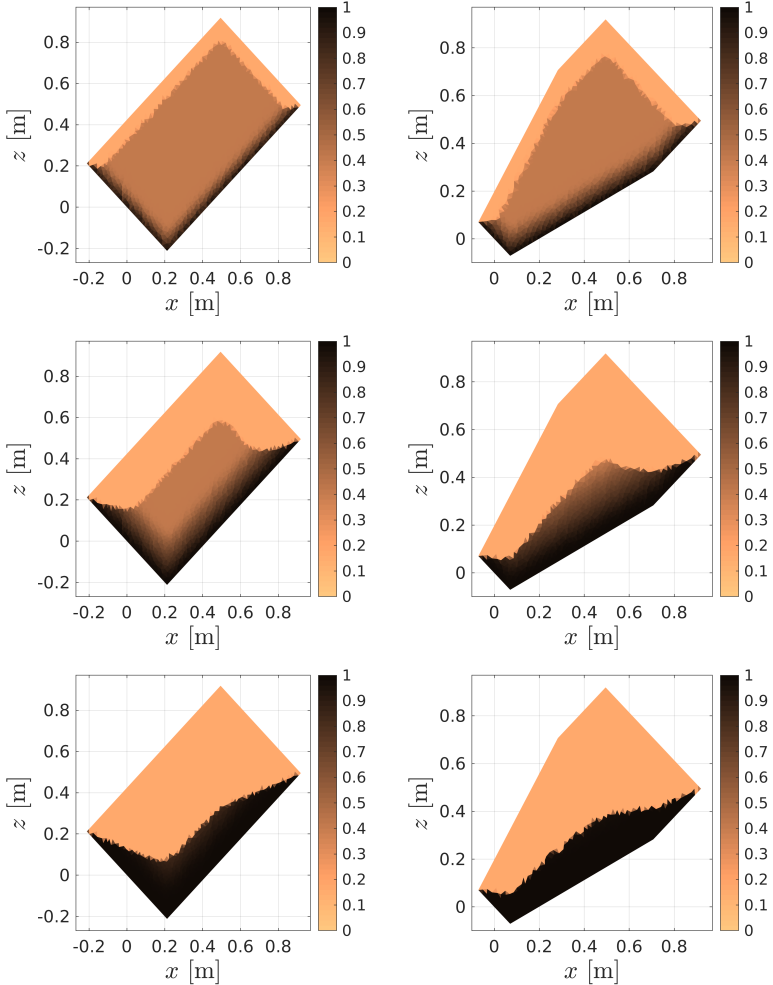


Figure 4.3: Volume fraction ϕ approximated by the finite volume schemes (4.10) in two different domains for the times $t = 35.3\text{s}$ (top), $t = 106.2\text{s}$ (middle) and $t = 318.6\text{s}$ (bottom). The simulation is made with the flux function (4.7) and angle of rotation $\theta = \pi/4$ with respect to a horizontal line.

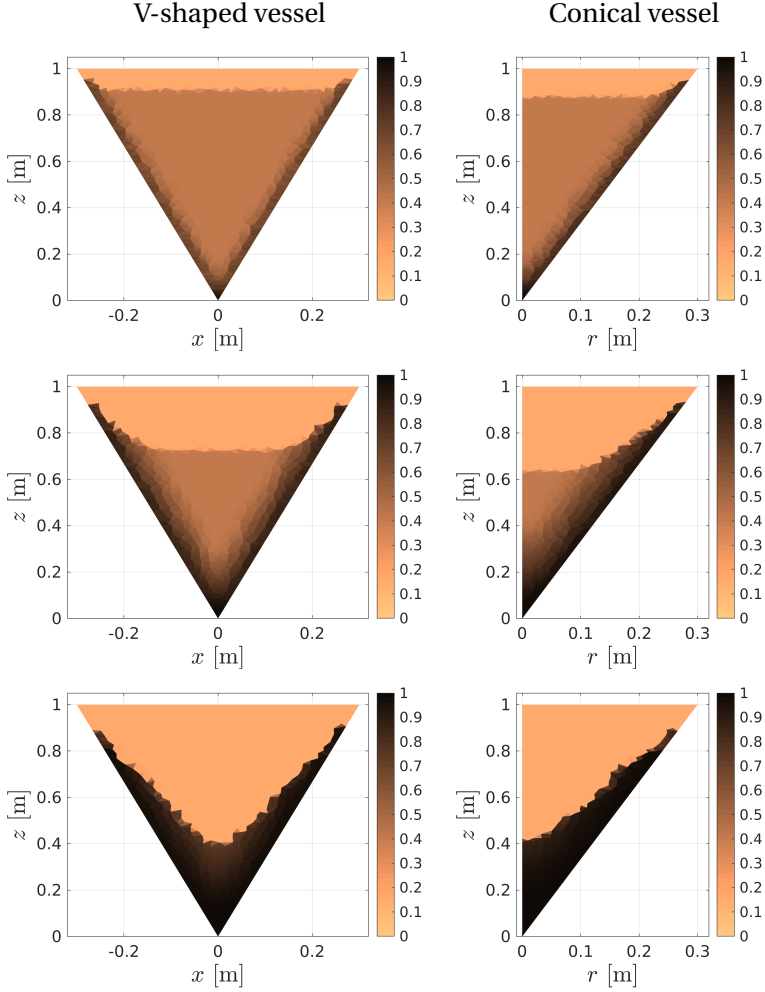


Figure 4.4: Simulation by (4.10) (left), and (4.11) (right) for the times $t = 35.3$ s (top), $t = 106.2$ s (middle) and $t = 318.6$ s (bottom). The simulation is made with the flux function (4.7) and angle of rotation $\theta = -\pi/2$ with respect to a horizontal line.

Figure 4.3 contains the simulation of two inclined vessel produced by (4.10) using the flux function (4.7), initial volume fraction $\phi_0 = 0.3$ and the angle of inclination with respect to the horizontal line $\theta = \pi/4$. As expected, in both simulations we can observe that the solid particles settle downward accumulating to the walls creating a non-horizontal bed whose shape depends on the vessel's geometry. Despite the assumption of $\mathbf{q} = \mathbf{0}$, the two dimensional simulation in the cylinder (left column in Figure 4.3) is in agreement with the ones presented in [19].

Figure 4.4 shows two simulations made with the schemes (4.10) and (4.11) with the domains presented in Figure 4.2. The flux function and initial volume fraction are the same as in the previous simulation (Figure 4.3) and the angle of rotation is $\theta = -\pi/2$. It can be observed from the simulation that the solid particles with the model equation (4.4) settle faster than the one with (4.1), nevertheless, with both models the particles stick to the walls generating a non-horizontal bed.

4.2 Simplified centrifugal settling in tubes

Another simplified multi-dimensional settling model that can also be simulated using a finite volume scheme, such that the ones presented in the previous section, is the process of centrifugal settling in tubes. The one-dimensional case of centrifugal sedimentation was presented in Paper III, where the entropy solution, numerical scheme and inverse problem of flux identification were studied. To differentiate from the two equations of the previous section, here the domain is denoted by Ω_R which is contained in the xz -plane. Let \mathbf{r} be the vector in the radial direction and ω the scalar angular speed. The model equation of this problem is given by

$$\partial_t \phi + \nabla \cdot (f(\phi)\omega^2 \mathbf{r}) = 0, \quad \mathbf{x} \in \Omega_R, \quad (4.12)$$

$$f(\phi)\omega^2 \mathbf{r} \cdot \mathbf{n} = 0, \quad \mathbf{x} \in \partial\Omega_R, \quad (4.13)$$

$$\phi(\mathbf{x}, 0) = \phi_0, \quad \phi_0 \in (0, 1). \quad (4.14)$$

The components of the vector \mathbf{r} coincide with the coordinates of the points, $\mathbf{r} = (x, z)$. Utilizing the same steps used to obtain (4.10) or (4.11), one can obtain the finite volume approximation of (4.12)

$$|K_i| \frac{\phi_i^{n+1} - \phi_i^n}{\Delta t} + \sum_{e \in \mathcal{E}_h(K_i)} \hat{F}_R^n \int_e \mathbf{r} \cdot \mathbf{n}_e ds = 0, \quad i = 1, \dots, |\mathcal{T}_h|. \quad (4.15)$$

where for an edge with nodes \mathbf{x}_1 and \mathbf{x}_2 , and middle point $\bar{\mathbf{r}}_e = (\mathbf{x}_1 + \mathbf{x}_2)/2$ the integral term can be computed by

$$\int_e \mathbf{r} \cdot \mathbf{n}_e ds = n_e^1 \int_e x ds + n_e^2 \int_e z ds = n_e^1 |e| \frac{x_1 + x_2}{2} + n_e^2 |e| \frac{z_1 + z_2}{2} = |e| \mathbf{n}_e \cdot \bar{\mathbf{r}}_e.$$

The numerical flux \hat{F}_R over an inner edge e between the two elements K_i and K_j is defined by

$$\hat{F}_R(\phi_i, \phi_j) := \begin{cases} -G(\phi_i, \phi_j) & \text{if } \bar{\mathbf{r}}_e \cdot \mathbf{n}_e \geq 0, \\ G(\phi_j, \phi_i) & \text{if } \bar{\mathbf{r}}_e \cdot \mathbf{n}_e < 0, \end{cases}$$

Figure (4.5) shows a simulation of centrifugal settling in a tube made with the scheme (4.15), with the nonlinear function

$$f(\phi) := C\phi(\exp(-r_V\phi) - \exp(-r_V)), \quad r_V = 4.5, \quad (4.16)$$

where C is chosen such that $\omega^2 C = 1$, and the same initial value as in the simulations presented in the previous subsection. As in the one-dimensional case, the particles tend to settle rapidly to the bottom wall forming a thick layer at $r = r_1$ followed by a diluted mixture at the middle of the tube. There exist a thin layer of solid particles that remain to the side wall of the vessel.

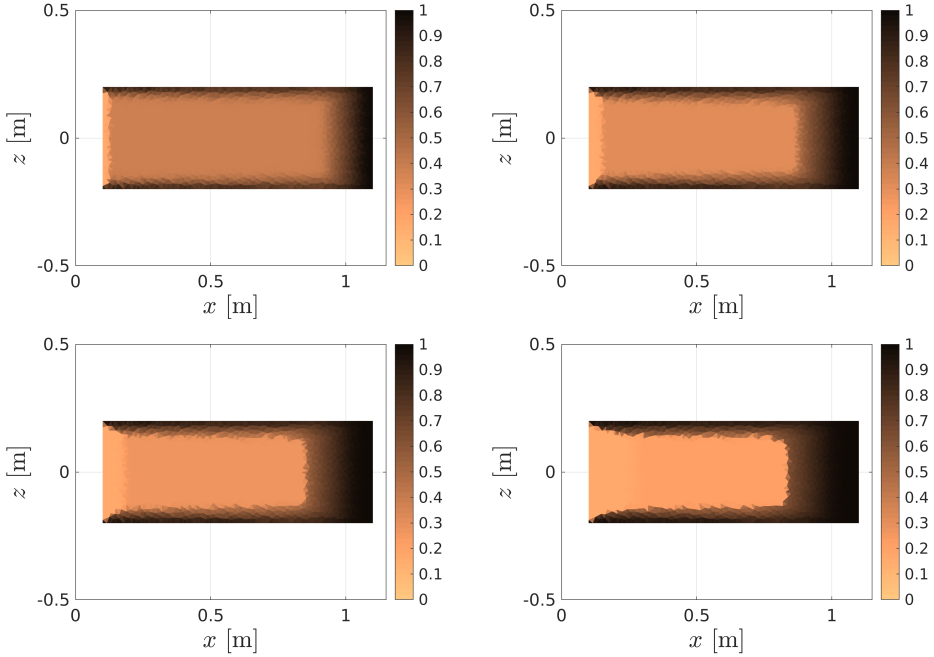


Figure 4.5: Simulation of centrifugation with a rotating tube obtained by the numerical scheme (4.15) at the times $t = 106.2$ s (top left), $t = 177$ s (top right), $t = 212.4$ s (bottom left) and $t = 248$ s (bottom right). The simulation is made with the function (4.16).

4.3 Fully coupled multidimensional settling

In the same way as (4.4), the model equations (2.6)–(2.8) (Model 1) with $\sigma_e \equiv 0$ can be adapted to axisymmetric domains Ω_a under the assumption of axisymmetry of the solutions. In this case the contribution of $\mathbf{q}\phi$ to the flux in (2.6) makes the numerical

approximation of (2.7)–(2.8) unavoidable. For a fix and constant ϕ , Equations (2.7)–(2.8) correspond to a Stokes system, which is often approximated by using Finite Element Methods. In [19] the authors have approximated Model 1 in cartesian grids by using a multiresolution finite volume scheme and splitting techniques. The numerical scheme for the simulation of SST in axisymmetric domains presented in [20] utilizes a vertex centered finite volume scheme combined with a stabilized discontinuous Galerkin method. A suitable choice for approximating the transport equation (2.6) is an interior penalty discontinuous Galerkin method, and for the coupled equations (2.7)–(2.8) a classical Finite Element approximation. To define the weak form of (2.6)–(2.8), the following weighted Sobolev spaces need to be introduced:

$$\begin{aligned} L_{0,1}^2(\Omega) &= \{q \in L_1^2(\Omega) : (q, 1)_1 = 0\}, \\ H_{\Gamma,1}^1(\Omega) &= \{w \in H_1^1(\Omega) : w = 0 \text{ on } \Gamma\}, \quad \Gamma \subseteq \partial\Omega, \end{aligned}$$

with inner product between two functions u, v given by

$$(u, v)_1 := \int_{\Omega} uvr \, dr dz,$$

and $L_1^2(\Omega)$ the space of functions whose induced norm $\|\cdot\|_1^2 := (\cdot, \cdot)_1$ is finite.

For ease of notation, the flux of Equation (2.6) is denoted by $\mathbf{F}(\phi, \mathbf{q}) := \phi \mathbf{q} - f(\phi) \mathbf{k}$. The boundary conditions considered for this model are

$$\mathbf{F}(\phi, \mathbf{q}) \cdot \mathbf{n} = 0, \quad (\mu(\phi) \boldsymbol{\varepsilon}(\mathbf{q}) - p \mathbf{I}) \cdot \mathbf{n} = 0, \quad \nabla p \cdot \mathbf{n} = 0 \quad \text{on } \partial\Omega,$$

and $\mathbf{q} = \mathbf{0}$ on $\Gamma_S := \partial\Omega \setminus \{r = 0\}$. The weak formulation of the axisymmetric version of (2.6)–(2.8) is the following: find $(\phi, \mathbf{q}, p) \in \mathbf{W} := H^1(\Omega) \times (H_{\Gamma_S,1}^1(\Omega))^2 \times L_{0,1}^2(\Omega)$ such that

$$(\partial_t \phi, \phi)_1 - (\mathbf{F}(\mathbf{q}, \phi), \nabla \phi)_1 = 0, \tag{4.17}$$

$$(\mu(\phi) \boldsymbol{\varepsilon}(\mathbf{q}), \boldsymbol{\varepsilon}(\mathbf{w}))_1 - (\nabla \cdot \mathbf{w}, p)_1 = -(\Delta \rho g \phi \mathbf{k}, \mathbf{w})_1, \tag{4.18}$$

$$(\nabla \cdot \mathbf{q}, \psi)_1 = 0, \tag{4.19}$$

for all $(\phi, \mathbf{w}, \psi) \in \mathbf{W}$, where ∇ here represents the axisymmetric gradient operator $\nabla_{\mathbf{a}}$ introduced in Section 4.1. The operator $\boldsymbol{\varepsilon}$ is defined by

$$\boldsymbol{\varepsilon}(\mathbf{q}) := \frac{1}{2} (\nabla \mathbf{q} + \nabla \mathbf{q}^T).$$

Let \mathbb{P}_k be the space of polynomial functions of degree less or equal than k , and consider the mesh triangulation \mathcal{T}_h described in Section 4.1. The finite element spaces

needed for the numerical formulation are:

$$\begin{aligned} S_h &:= \{s \in L^2_1(\Omega) : s|_{\partial K} \in \mathbb{P}_0(\Omega), \forall K \in \mathcal{T}_h\}, \\ \mathbf{V}_h &:= \{\mathbf{v} \in (H^2_{\Gamma,S,1}(\Omega))^2 \cap (C_0(\overline{\Omega}))^2 : \mathbf{v}|_{\partial K} \in (\mathbb{P}_1(\Omega))^2, \forall K \in \mathcal{T}_h\}, \\ Q_h &:= \{p \in L^2_{0,1}(\Omega) \cap C_0(\overline{\Omega}) : p|_{\partial K} \in \mathbb{P}_1(\Omega), \forall K \in \mathcal{T}_h\}. \end{aligned}$$

Where ϕ , \mathbf{q} and p are approximated by $\phi_h^n \in S_h$, $\mathbf{q}_h^n \in \mathbf{V}_h$ and $p_h^n \in Q_h$, respectively. Following the ideas of [20], the fully discrete approximation of Equation (4.17) based in the Discontinuous Galerkin interior penalty method is

$$\frac{(\phi_h^{n+1} - \phi_h^n, \varphi)_1}{\Delta t} + \sum_{e \in \mathcal{E}_h} (\hat{\mathbf{F}}(\mathbf{q}_h^{n+1}, \phi_h^{n+1}) \cdot \mathbf{n}_e, [[\nabla \varphi]])_{1,e} + \sum_{e \in \mathcal{E}_h} \frac{\kappa^\phi}{h_e^2} ([[\phi_h^{n+1}]], [[\varphi]])_{1,e} = 0, \quad (4.20)$$

for all $\varphi \in S_h$, where the operators $(\cdot, \cdot)_{1,e}$ and $[[\cdot]]$ are the inner product and jump over the edge e , respectively, and the numerical flux $\hat{\mathbf{F}}$ is given by

$$\hat{\mathbf{F}}(\mathbf{q}_h^n, \phi_h^n) \cdot \mathbf{n}_e := \left[\left[\frac{\phi_h^n}{2} (\mathbf{F}(\mathbf{q}_h^n, \phi_h^n) \cdot \mathbf{n}_e + |\mathbf{F}(\mathbf{q}_h^n, \phi_h^n) \cdot \mathbf{n}_e|) \right] \right].$$

The pair $(\mathbf{q}^{n+1}, p^{n+1})$ is obtained by solving the system:

$$2(\mu(\phi_h^{n+1})\boldsymbol{\varepsilon}(\mathbf{q}_h^{n+1}), \boldsymbol{\varepsilon}(\mathbf{w}))_1 - (p_h^{n+1}, \nabla \cdot \mathbf{w})_1 + I_{\mathbf{q}} = -(\Delta \rho g \phi_h^{n+1} \mathbf{k}, \mathbf{w})_1, \quad (4.21)$$

$$(\psi, \nabla \cdot \mathbf{q}_h^{n+1})_1 + \sum_{K \in \mathcal{T}_h} \frac{h_K^2}{\kappa^p} (\nabla p_h^{n+1} + \Delta \rho g \phi_h^{n+1} \mathbf{k}, \nabla \psi)_{1,K} = 0 \quad (4.22)$$

for all $\mathbf{w} \in \mathbf{V}_h$, $\psi \in Q_h$, where the term $I_{\mathbf{q}}$ is defined by

$$I_{\mathbf{q}} := \sum_{e \in \mathcal{E}_h} \frac{4h_e}{\kappa^U} ([[\mu(\phi_h^{n+1})\boldsymbol{\varepsilon}(\mathbf{q}_h^{n+1}) \cdot \mathbf{n}_e]], [[\mu(\phi_h^{n+1})\boldsymbol{\varepsilon}(\mathbf{w}) \cdot \mathbf{n}_e]])_{1,e}.$$

The constants κ^ϕ , $\kappa^{\mathbf{q}}$ and κ^p are positive stabilization parameters. Equation (4.20) is implicit in time and a non-linear solver method is needed, e.g., Newton-Raphson's method. The condition $(p, 1)_1 = 0$ can be added to (4.21)–(4.22) by means of lagrange multipliers.

The numerical scheme proposed here utilizes several ingredients from [20], nevertheless it is fully implicit in time and no dual mesh is needed. The numerical scheme has been implemented in FEniCS [88] (version 2019) with the following constants and constitutive functions: $\Delta \rho = 50 \text{ kg/m}^3$, homogeneous initial volume fraction $\phi_0 = 0.3$, velocity and viscosity functions given by

$$\begin{aligned} v(\phi) &= 0.08 (\exp(-4.5\phi) - \exp(-4.5)), \\ \mu(\phi) &= \left(1 - \frac{\phi}{1.3} \right)^{-2.5}, \end{aligned}$$

constants $\kappa^\phi = 10^{-5}$, $\kappa^p = 2\mu(1)$, $\kappa^U = \mu(1)$ and $\Delta t = 0.5\text{s}$. The mesh is generated by *mshr*, the mesh generator of FEniCS, and the non-linear solver chosen is the Newton-Raphson's method. The simulation of the sedimentation in a conical vessel produced by (4.20) and (4.21)–(4.22) is presented in Figures 4.6 and 4.7, where the volume fraction and the norm of the volume average velocity in six different time points are shown.

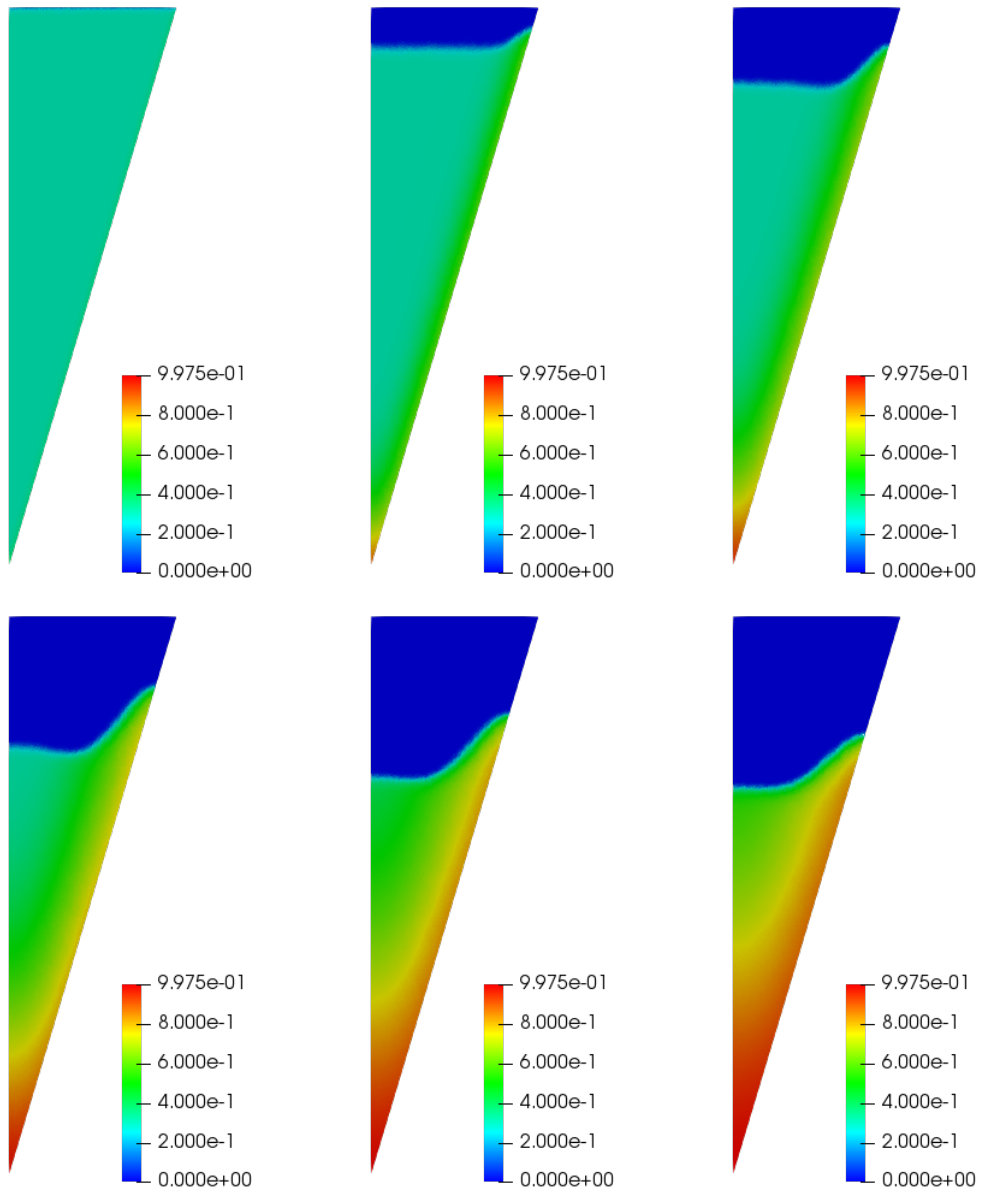


Figure 4.6: Sedimentation in a cone: Simulated volume fraction of solid particles ϕ produced by the numerical scheme (4.20) and (4.21)–(4.22) for six different time points.

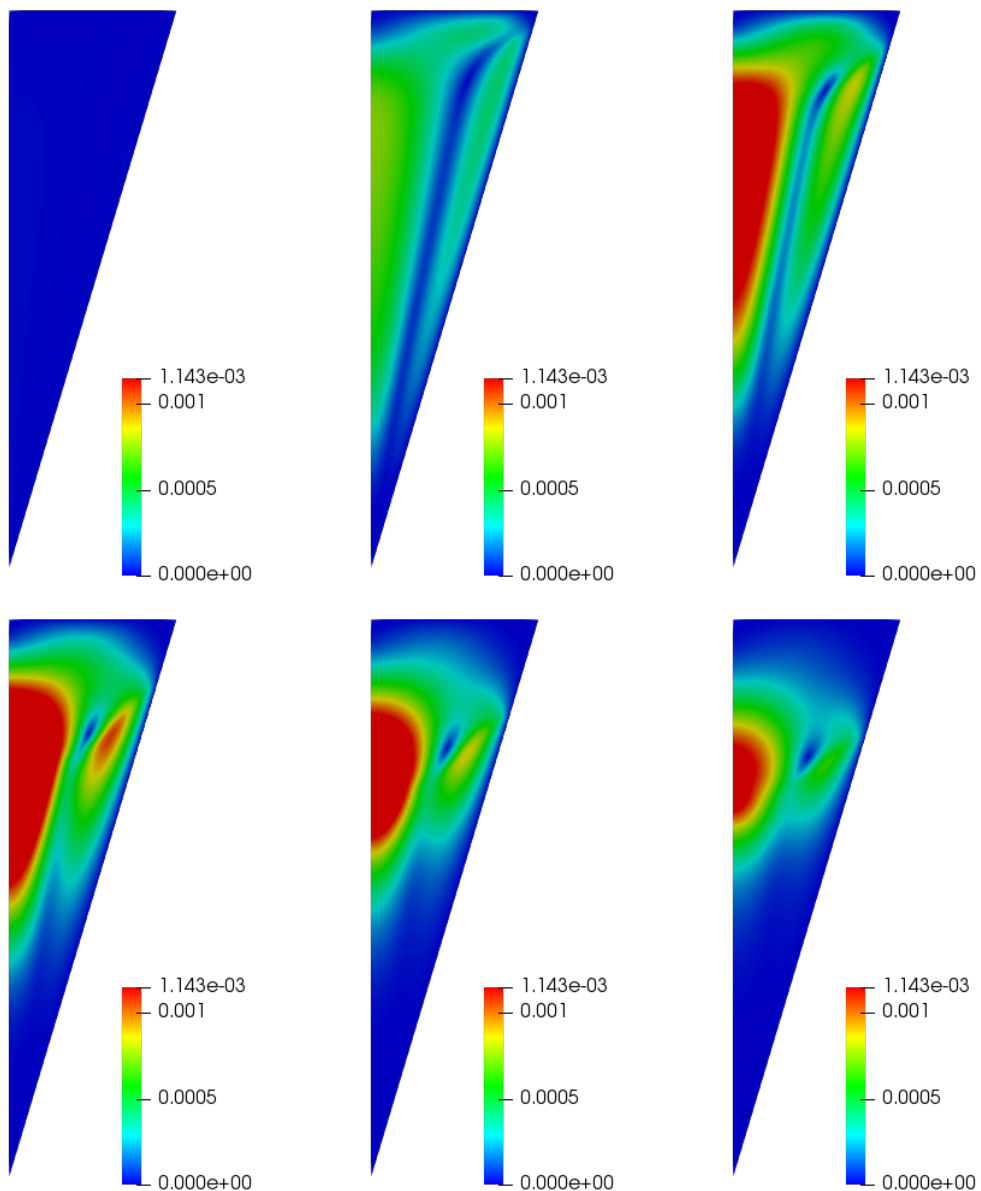


Figure 4.7: Sedimentation in a cone: Simulated norm of the volume average velocity $\|\mathbf{q}\|$ produced by the numerical scheme (4.20) and (4.21)–(4.22) for six different time points.

Conclusions

This thesis is based in mathematical modeling of sedimentation processes with research topics divided into three parts: Entropy solutions and inverse problem, numerical schemes and simulation models, and validation and dissemination.

In the first part, two problems are studied, the batch sedimentation in vessels with varying cross-sectional area and the centrifugal settling. Both are modeled by first-order quasi-linear hyperbolic PDEs, Equations (3.1) and (3.6), respectively. Detailed constructions of the entropy solutions in both problems were made by using the method of characteristics. The knowledge obtained about the relations between the characteristics and discontinuities led to the definition and (partial) solution of the inverse problem of flux identification. Two new methods of flux identification based on the solutions of the inverse problems are presented. These methods represent a significant improvement, at least theoretically, compared to previous works [3, 8, 43] in terms of the portion of flux identified, and also that only one experiment and no prescribed functional expressions are needed. Constructed entropy solutions can be used as test cases for numerical schemes. A limitation in this part is that compression effects are not considered. These effects are often simulated by a second-order degenerate term, adding a level of complication in the construction of the entropy solutions, and in consequence, to the inverse problem of flux identification. The work done in this part of the thesis can be extended in different ways, for example to the case of a more general flux functions, including more than one inflection point, or for the case of the inverse problem of (3.1), to a more general cross-sectional area function.

The second part contains the modeling and numerical simulation of secondary settling tanks (SSTs) with varying cross-sectional area, where continuous sedimentation occurs with or without reactions, depending on the plant and application. Furthermore, sequencing batch reactors (SBRs) in vessels with varying cross-sectional area are modeled by means of PDEs and simulated. These problems are of interest for the wastewater treatment community, where steady-state simulations are more

common than transient solutions connected to the mathematical theory of PDEs. The non-reactive settling is modeled by (2.21), the reactive case by (3.10)–(3.12) and the SBR by (3.13)–(3.15). The three sedimentation processes are modeled by PDEs that share many features; non-linear fluxes, second-order degenerated terms and non-linear coefficient functions. The vectorial way in which the PDE models in the reactive-settling case and SBR are written allows the application in cases where there are several substrates and reactions are taking place, for example in the established activated sludge models for biological reactions in wastewater treatment (ASM_x) [72]. Detailed numerical schemes are introduced to approximate the three PDE models. In the case of Equation (2.21), the approximation is carried out by an extension of the numerical scheme developed for the Bürger-Diehl model [12] to the varying cross-sectional area case. One of the novelties is an improved CFL condition where simulations can be obtained more efficiently than with previous methods. The reactive case, system (3.10)–(3.12), is approximated mainly by an upwind scheme leading to a method-of-lines formulation (semi-discrete scheme), and an extension of it is used for the approximation of system (3.13)–(3.15) in the application to SBRs. In the three cases, the schemes capture the nature of the PDEs properly (discontinuities), they are proven to be monotone and the approximated solutions are physically relevant. In the three problems, simulations have been made to visualize, among others, the influences of the cross-sectional area in the sedimentation process, the versatility of soluble diffusion effects, and approximation of the moving boundary for the case of the SBR problem. The numerical schemes introduced in this part are all first-order accurate, and could be improved to a second- or higher-order accuracy scheme, by for instance, utilizing high-order weighted essentially non-oscillatory reconstructions combined with strong stability-preserving Runge–Kutta time schemes.

In the third part, the flux identification method in conical vessels developed previously was tested and successfully validated with experimental data of batch settling in cones. The validation shows that with one experiment only, the measurement of the sludge blanket level is enough to determine almost the entire flux function. It should be mentioned, however, that experiments with mineral powders carried out with collaborators did not give as good results with the method, which can be partially explained by external conditions (temperature) or two-dimensional effects. The later motivates the two-dimensional simulations presented in Chapter 4, which could be a starting-point for future research to improve the identification method. Nevertheless, the review of flux identification methods in Paper VIII reveals the advantages of the methods developed in this thesis over previous methods from the literature.

Bibliography

- [1] Adimurthi, J. Jaffré, and G. D. Veerappa Gowda. Godunov-type methods for conservation laws with a flux function discontinuous in space. *SIAM J. Num. Anal.*, 42(1):179–208, 2004.
- [2] U. Attir and M. M. Denn. Dynamics and control of the activated sludge wastewater process. *AIChE J.*, 24:693–698, 1978.
- [3] F. Betancourt, R. Bürger, S. Diehl, and C. Mejías. Advanced methods of flux identification for clarifier–thickener simulation models. *Minerals Eng.*, 63:2–15, 2014.
- [4] R. Bürger, J. Careaga, S. Diehl, C. Mejías, I. Nopens, and P. A. Vanrolleghem. Simulations of reactive settling of activated sludge with a reduced biokinetic model. *Computers Chem. Eng.*, 92:216–229, 2016.
- [5] R. Bürger, F. Concha, and F. M. Tiller. Applications of the phenomenological theory to several published experimental cases of sedimentation processes. *Chem. Eng. J.*, 80:105–117, 2000.
- [6] R. Bürger, A. Coronel, and M. Sepúlveda. On an upwind difference scheme for strongly degenerate parabolic equations modelling the settling of suspensions in centrifuges and non-cylindrical vessels. *Appl. Num. Math.*, 56:1397–1417, 2006.
- [7] R. Bürger, J. J. R. Damasceno, and K. H. Karlsen. A mathematical model for batch and continuous thickening of flocculated suspensions in vessels with varying cross-section. *Int. J. Miner. Process.*, 73:183–208, 2004.
- [8] R. Bürger and S. Diehl. Convexity-preserving flux identification for scalar conservation laws modelling sedimentation. *Inverse Problems*, 29(4):045008, 2013.

- [9] R. Bürger, S. Diehl, S. Farås, and I. Nopens. On reliable and unreliable numerical methods for the simulation of secondary settling tanks in wastewater treatment. *Computers Chem. Eng.*, 41:93–105, 2012.
- [10] R. Bürger, S. Diehl, S. Farås, I. Nopens, and E. Torfs. A consistent modelling methodology for secondary settling tanks: A reliable numerical method. *Water Sci. Tech.*, 68(1):192–208, 2013.
- [11] R. Bürger, S. Diehl, and C. Mejías. A difference scheme for a degenerating convection-diffusion-reaction system modelling continuous sedimentation. *ESAIM: Math. Modelling Num. Anal.*, 52:365–392, 2018.
- [12] R. Bürger, S. Diehl, and I. Nopens. A consistent modelling methodology for secondary settling tanks in wastewater treatment. *Water Res.*, 45(6):2247–2260, 2011.
- [13] R. Bürger, S. Evje, and K. H. Karlsen. On strongly degenerate convection-diffusion problems modeling sedimentation-consolidation processes. *J. Math. Anal. Appl.*, 247:517–556, 2000.
- [14] R. Bürger, S. Evje, K. H. Karlsen, and K.-A. Lie. Numerical methods for the simulation of the settling of flocculated suspensions. *Chem. Eng. J.*, 80:91–104, 2000.
- [15] R. Bürger, K. H. Karlsen, C. Klingenberg, and N. H. Risebro. A front tracking approach to a model of continuous sedimentation in ideal clarifier-thickener units. *Nonl. Anal. Real World Appl.*, 4:457–481, 2003.
- [16] R. Bürger, K. H. Karlsen, N. H. Risebro, and J. D. Towers. Monotone difference approximations for the simulation of clarifier-thickener units. *Comput. Vis. Sci.*, 6:83–91, 2004.
- [17] R. Bürger, K. H. Karlsen, N. H. Risebro, and J. D. Towers. Well-posedness in BV_t and convergence of a difference scheme for continuous sedimentation in ideal clarifier-thickener units. *Numer. Math.*, 97:25–65, 2004.
- [18] R. Bürger, K. H. Karlsen, and J. D. Towers. A model of continuous sedimentation of flocculated suspensions in clarifier-thickener units. *SIAM J. Appl. Math.*, 65:882–940, 2005.
- [19] R. Bürger, R. Ruiz-Baier, K. Schneider, and H. Torres. A multiresolution method for the simulation of sedimentation in inclined channels. *Int. J. Numer. Anal. Model.*, 9:479–504, 2012.

- [20] R. Bürger, R. Ruiz-Baier, and H. Torres. A stabilized finite volume element formulation for sedimentation-consolidation processes. *SIAM J. Sci. Comput.*, 34:B265–B289, 2012.
- [21] R. Bürger and W. L. Wendland. Entropy boundary and jump conditions in the theory of sedimentation of with compression. *Math. Meth. Appl. Sci.*, 21:865–882, 1998.
- [22] R. Bürger and W. L. Wendland. Existence, uniqueness, and stability of generalized solutions of an initial-boundary value problem for a degenerating quasi-linear parabolic equation. *J. Math. Anal. Appl.*, 218:207–239, 1998.
- [23] R. Bürger, W. L. Wendland, and F. Concha. Model equations for gravitational sedimentation-consolidation processes. *Z. Angew. Math. Mech.*, 80:79–92, 2000.
- [24] M. C. Bustos and F. Concha. Boundary conditions for the continuous sedimentation of ideal suspensions. *AIChE J.*, 38(7):1135–1138, 1992.
- [25] M. C. Bustos, F. Concha, R. Bürger, and E. M. Tory. *Sedimentation and Thickening: Phenomenological Foundation and Mathematical Theory*. Kluwer Academic Publishers, Dordrecht, The Netherlands, 1999.
- [26] M. C. Bustos, F. Concha, and W. Wendland. Global weak solutions to the problem of continuous sedimentation of an ideal suspension. *Math. Meth. Appl. Sci.*, 13:1–22, 1990.
- [27] M. C. Bustos, F. Paiva, and W. Wendland. Control of continuous sedimentation as an initial and boundary value problem. *Math. Meth. Appl. Sci.*, 12:533–548, 1990.
- [28] C. Castro and E. Zuazua. Flux identification for 1-d scalar conservation laws in the presence of shocks. *Math. Comp.*, 80(276):2025–2070, 2011.
- [29] J.-Ph. Chancelier, M. Cohen de Lara, and F. Pacard. Analysis of a conservation PDE with discontinuous flux: A model of settler. *SIAM J. Appl. Math.*, 54(4):954–995, 1994.
- [30] F. Concha and R. Bürger. A century of research in sedimentation and thickening. *KONA Powder and Particle*, 20:38–70, 2002.
- [31] F. Concha and R. Bürger. Thickening in the 20th century: A historical perspective. *Miner. Metall. Proc.*, 20:57–67, 2003.

- [32] A. Coronel, F. James, and M. Sepúlveda. Numerical identification of parameters for a model of sedimentation processes. *Inverse Problems*, 19(4):951–972, 2003.
- [33] P. J. T. Dankers and J. C. Winterwerp. Hindered settling of mud flocs: Theory and validation. *Continent. Shelf Res.*, 27(14):1893–1907, 2007.
- [34] B. De Clercq, A. Vanderhasselt, B. Vanderhaegen, L. N. Hopkins, and P. A. Vanrolleghem. A model-based evaluation of control strategies for a clarifier at an industrial wastewater treatment plant. In *Proceedings 8th IAWQ Conference on Design, Operation and Economics of Large Wastewater Treatment Plants*, pages 452–455, Budapest, Hungary, September 6-9, 1999.
- [35] J. De Clercq, M. Devisscher, I. Boonen, J. Defrancq, and P. A. Vanrolleghem. Analysis and simulation of the sludge profile dynamics in a full-scale clarifier. *J. Chem. Tech. Biotechnol.*, 80(5):523–530, 2005.
- [36] S. Diehl. On scalar conservation laws with point source and discontinuous flux function. *SIAM J. Math. Anal.*, 26(6):1425–1451, 1995.
- [37] S. Diehl. A conservation law with point source and discontinuous flux function modelling continuous sedimentation. *SIAM J. Appl. Math.*, 56(2):388–419, 1996.
- [38] S. Diehl. Dynamic and steady-state behavior of continuous sedimentation. *SIAM J. Appl. Math.*, 57(4):991–1018, 1997.
- [39] S. Diehl. On boundary conditions and solutions for ideal clarifier-thickener units. *Chem. Eng. J.*, 80:119–133, 2000.
- [40] S. Diehl. Operating charts for continuous sedimentation I: Control of steady states. *J. Eng. Math.*, 41:117–144, 2001.
- [41] S. Diehl. Operating charts for continuous sedimentation II: Step responses. *J. Eng. Math.*, 53:139–185, 2005.
- [42] S. Diehl. Operating charts for continuous sedimentation III: Control of step inputs. *J. Eng. Math.*, 54:225–259, 2006.
- [43] S. Diehl. Estimation of the batch-settling flux function for an ideal suspension from only two experiments. *Chem. Eng. Sci.*, 62:4589–4601, 2007.
- [44] S. Diehl. Operating charts for continuous sedimentation IV: Limitations for control of dynamic behaviour. *J. Eng. Math.*, 60:249–264, 2008.

- [45] S. Diehl. A regulator for continuous sedimentation in ideal clarifier-thickener units. *J. Eng. Math.*, 60:265–291, 2008.
- [46] S. Diehl. A uniqueness condition for nonlinear convection-diffusion equations with discontinuous coefficients. *J. Hyperbolic Differential Equations*, 6:127–159, 2009.
- [47] S. Diehl. Shock-wave behaviour of sedimentation in wastewater treatment: A rich problem. In K. Åström, L.-E. Persson, and S. D. Silvestrov, editors, *Analysis for Science, Engineering and Beyond*, volume 6 of *Springer Proceedings in Mathematics*, pages 175–214. Springer Berlin Heidelberg, 2012.
- [48] S. Diehl and S. Farås. Fundamental nonlinearities of the reactor-settler interaction in the activated sludge process. *Water Sci. Tech.*, 66(1):28–35, 2012.
- [49] S. Diehl and S. Farås. A reduced-order ODE-PDE model for the activated sludge process in wastewater treatment: Classification and stability of steady states. *Math. Models Meth. Appl. Sci.*, 23(3):369–405, 2013.
- [50] S. Diehl and U. Jeppsson. A model of the settler coupled to the biological reactor. *Water Res.*, 32(2):331–342, 1998.
- [51] S. Diehl and N.-O. Wallin. Scalar conservation laws with discontinuous flux function: II. On the stability of the viscous profiles. *Commun. Math. Phys.*, 176:45–71, 1996.
- [52] D. A. Drew and S. L. Passman. *Theory of Multicomponent Fluids*, volume 135. Springer-Verlag, New York, 1999.
- [53] G. A. Ekama and P. Marais. Assessing the applicability of the 1D flux theory to full-scale secondary settling tank design with a 2D hydrodynamic model. *Water Res.*, 38:495–506, 2004.
- [54] B. Engquist and S. Osher. One-sided difference approximations for nonlinear conservation laws. *Math. Comput.*, 36:321–351, 1981.
- [55] G. Esposito, M. Fabbicino, and F. Pirozzi. Four-substrate design model for single sludge predenitrification system. *J. Environ. Eng.*, 129(5):394–401, 2003.
- [56] S. Evje and K. H. Karlsen. Monotone difference approximations of BV solutions to degenerate convection-diffusion equations. *SIAM J. Numer. Anal.*, 37:1838–1860, 2000.
- [57] L. Fernandes, K.J. Kennedy, and Z. Ning. Dynamic modelling of substrate degradation in sequencing batch anaerobic reactors (SBAR). *Water Res.*, 27(11):1619–1628, 1993.

- [58] E. M. Fernández-Berdaguer and G. B. Savioli. An inverse problem arising from the displacement of oil by water in porous media. *Appl. Num. Math.*, 59(10):2452–2466, 2009.
- [59] J. Ferrer, A. Seco, and J. Serralta. DESASS: A software tool for designing, simulating and optimising WWTPs. *Environ. Model. Software*, 23(1):19–27, 2008.
- [60] X. Flores-Alsina, K.V. Gernaey, and U. Jeppsson. Benchmarking biological nutrient removal in wastewater treatment plants: Influence of mathematical model assumptions. *Water Sci. Tech.*, 65(8):1496–1505, 2012.
- [61] D. Gao, Y. Peng, and W.-M. Wu. Kinetic model for biological nitrogen removal using shortcut nitrification-denitrification process in sequencing batch reactor. *Environ. Sci. Technol.*, 44(13):5015–5021, 2010.
- [62] H. Gao and M. K. Stenstrom. Development and applications in computational fluid dynamics modeling for secondary settling tanks over the last three decades: A review. *Water Environ. Res.*, 92(6):796–820, 2019.
- [63] P. Garrido, R. Burgos, F. Concha, and R. Bürger. Software for the design and simulation of gravity thickeners. *Miner. Eng.*, 16:85–92, 2003.
- [64] P. Garrido, R. Burgos, F. Concha, and R. Bürger. Settling velocities of particulate systems: 13. A simulator for batch and continuous sedimentation of flocculated suspensions. *Int. J. Miner. Process.*, 73:131–144, 2004.
- [65] K. V. Gernaey, U. Jeppsson, D. J. Batstone, and P. Ingildsen. Impact of reactive settler models on simulated WWTP performance. *Water Sci. Tech.*, 53(1):159–167, 2006.
- [66] K. V. Gernaey, U. Jeppsson, P. A. Vanrolleghem, and J. B. Copp. *Benchmarking of control strategies for wastewater treatment plants*. IWA Scientific and Technical Report No. 23. IWA Publishing, London, UK, 2014.
- [67] K. V. Gernaey, M. C. M. van Loosdrecht, M. Henze, M. Lind, and S. B Jørgensen. Activated sludge wastewater treatment plant modelling and simulation: state of the art. *Environ. Model. Software*, 19(9):763–783, 2004.
- [68] T. Gimse and N. H. Risebro. Solution of the Cauchy problem for a conservation law with a discontinuous flux function. *SIAM J. Math. Anal.*, 23(3):635–648, 1992.
- [69] W. Gujer. *Systems Analysis for Water Technology*. Springer Berlin Heidelberg, 2008.

- [70] K. Gustavsson and J. Ooppelstrup. Consolidation of concentrated suspensions – numerical simulations using a two-phase fluid model. *Comput. Visual. Sci.*, 3(1–2):39–45, 2000.
- [71] M. Henze, C. P. L. Grady, W. Gujer, G. V. R. Marais, and T. Matsuo. *Activated Sludge Model No. 1*. Technical Report 1, IAWQ, London, UK, 1987.
- [72] M. Henze, Gujer, T. W., Mino, and M. C. M. van Loosdrecht. *Activated Sludge Models ASM1, ASM2, ASM2d and ASM3*, volume IWA Scientific and Technical Report No. 9. IWA Publishing, London, UK, 2000.
- [73] H. Holden and N. H. Risebro. *Front Tracking for Hyperbolic Conservation Laws*. Second Edition, Springer Verlag, Berlin, 2015.
- [74] G. Ibrahim and A.E. Abasaheed. Modelling of sequencing batch reactors. *Water Res.*, 29(7):1761–1766, 1995.
- [75] E. Iritani, T. Hashimoto, and N. Katagiri. Gravity consolidation-sedimentation behaviors of concentrated TiO₂ suspension. *Chem. Eng. Sci.*, 64(21):4414–4423, 2009.
- [76] I. Irizar. A mathematical framework for optimum design and operation of SBR processes. *J. Water Process Eng.*, 39:101703, 2021.
- [77] R.L. Irvine, T.P. Fox, and R.O. Richter. Investigation of fill and batch periods of sequencing batch biological reactors. *Water Res.*, 11(8):713–717, 1977.
- [78] U. Jeppsson and S. Diehl. An evaluation of a dynamic model of the secondary clarifier. *Water Sci. Tech.*, 34(5–6):19–26, 1996.
- [79] H. Kang and K. Tanuma. Inverse problems for scalar conservation laws. *Inverse Problems*, 21(3):1047–1059, 2005.
- [80] A. A. Kazmi, M. Fujita, and H. Furumai. Modeling effect of remaining nitrate on phosphorus removal in sbr. *Water Sci. Tech.*, 43(3):175–182, 2001.
- [81] A. A. Kazmi and H. Furumai. Field investigations on reactive settling in an intermittent aeration sequencing batch reactor activated sludge process. *Water Sci. Technol.*, 41(1):127–135, 2000.
- [82] A. A. Kazmi and N. Furumai. A simple settling model for batch activated sludge process. *Water Sci. Tech.*, 42(3-4):9–16, 2000.
- [83] J. Keller and Z. Yuan. Combined hydraulic and biological modelling and full-scale validation of SBR process. *Water Sci. Tech.*, 45(6):219–228, 2002.

- [84] G. J. Kynch. A theory of sedimentation. *Trans. Faraday Soc.*, 48:166–176, 1952.
- [85] R. J. LeVeque. *Numerical Methods for Conservation Laws*. Birkhäuser Verlag, 1992.
- [86] B. Li and M. K. Stenstrom. Construction of analytical solutions and numerical methods comparison of the ideal continuous settling model. *Computers Chem. Eng.*, 80:211–222, 2015.
- [87] Dan Li, Hai Zhen Yang, and Xiao Feng Liang. Application of Bayesian networks for diagnosis analysis of modified sequencing batch reactor. *Adv. Mater. Res.*, 610-613:1139–1145, 2012.
- [88] A. Logg, K.-A. Mardal, and G. Wells, editors. *Automated Solution of Differential Equations by the Finite Element Method*. Springer Berlin Heidelberg, 2012.
- [89] D. Massé. Comprehensive model of anaerobic digestion of swine manure slurry in a sequencing batch reactor. *Water Res.*, 34(12):3087–3106, 2000.
- [90] O. A. Oleinik. Uniqueness and stability of the generalized solution of the Cauchy problem for a quasi-linear equation. *Uspekhi Mat. Nauk*, 14:165–170, 1959. *Amer. Math. Soc. Trans. Ser. 2*, 33, (1964), pp. 285–290.
- [91] G. S. Ostace, V. M. Cristea, and P. S. Agachi. Evaluation of different control strategies of the waste water treatment plant based on a modified activated sludge model no. 3. *Environ. Eng. Management J.*, 11(1):147–164, 2012.
- [92] C. A. Petty. Continuous sedimentation of a suspension with a nonconvex flux law. *Chem. Eng. Sci.*, 30:1451–1458, 1975.
- [93] R. Ruiz-Baier R. Bürger and H. Torres. Numerical solution of a multidimensional sedimentation problem using finite volume-element methods. *App. Num. Math.*, 95(280):280–291, 2015.
- [94] R. Ruiz-Baier and I. Lunati. Mixed finite element – discontinuous finite volume element discretization of a general class of multicontinuum models. *J. Comp. Phys.*, 322:666–688, 2016.
- [95] R. Saagi, X. Flores-Alsina, S. Kroll, K. V. Gernaey, and U. Jeppsson. A model library for simulation and benchmarking of integrated urban wastewater systems. *Environ. Modelling & Software*, 93:282–295, 2017.
- [96] U. Schaflinger. Experiment on sedimentation beneath downward-facing inclined walls. *Int. J. Multiphase Flow*, 11(2):189–199, 1985.

- [97] U. Schaflinger. Influence of nonuniform particle size on settling downward-facing inclined walls. *Int. J. Multiphase Flow*, 11(6):783–796, 1985.
- [98] W. Schneider. Kinematic-wave theory of sedimentation beneath inclined walls. *J. Fluid Mech.*, 120:323–346, 1982.
- [99] W. Schneider. On the one-dimensional flow approximation in sedimentation processes. In: *Gyr A., Kinzelbach W. (eds) Sedimentation and Sediment Transport*. Springer, Dordrecht, pages 127–130, 2003.
- [100] H. Steinour. Rate of sedimentation. *Ind. Eng. Chem.*, 36(9):840–847, 1944.
- [101] H. Steinour. Rate of sedimentation: Concentrated flocculated suspensions of powders. *Ind. Eng. Chem.*, 36(10):901–907, 1944.
- [102] H. Steinour. Rate of sedimentation: Nonflocculated suspensions of uniform spheres. *Ind. Eng. Chem.*, 36(7):618–624, 1944.
- [103] I. Takács, G. G. Patry, and D. Nolasco. A dynamic model of the clarification-thickening process. *Water Res.*, 25(10):1263–1271, 1991.
- [104] E. Torfs. *Different settling regimes in secondary settling tanks: experimental process analysis, model development and calibration*. PhD thesis, Ghent University, Belgium, 2015.
- [105] E. Torfs, S. Balemans, F. Locatelli, S. Diehl, R. Bürger, J. Laurent, P. François, and I. Nopens. On constitutive functions for hindered settling velocity in 1-d settler models: Selection of appropriate model structure. *Water Res.*, 110:38–47, 2017.
- [106] C. Truesdell. *Rational thermodynamics*. Springer Verlag, New York, 1984.
- [107] S. Velmurugan, W. W. Clarkson, and J. N. Veenstra. Model-based design of sequencing batch reactor for removal of biodegradable organics and nitrogen. *Water Env. Res.*, 82(5):462–474, 2010.
- [108] D. A. White and N. Verdone. Numerical modelling of sedimentation processes. *Chem. Eng. Sci.*, 55:2213–2222, 2000.
- [109] A. Zeidan, S. Rohani, and Z. Bassi. BioSys: Software for wastewater treatment simulation. *Adv. Eng. Software*, 34:539–549, 2003.

Papers I to VIII can be found in the printed version.